LBL-16806
UC-94c

Lawrence Berkeley Laboratory

UNIVERSITY OF CALIFORNIA

RECEIVED
LAWRENCE
BERKELEY LABORATORY
JAN 17 1984
LIBRARY AND
DOCUMENTS SECTION

APPLIED SCIENCE DIVISION

THERMODYNAMIC FRAMEWORK FOR ESTIMATING THE EFFICIENCIES OF ALKALINE BATTERIES
FINAL REPORT

B. Pound, B. Sundararaj, R.P. Singh,
and D.D. Macdonald

October 1983

For Reference

Not to be taken from this room

APPLIED SCIENCE
DIVISION

LBL-16806 c.1

Prepared for the U.S. Department of Energy under Contract DE-AC03-76SF00098

DISCLAIMER

This document was prepared as an account of work sponsored by the United States Government. While this document is believed to contain correct information, neither the United States Government nor any agency thereof, nor the Regents of the University of California, nor any of their employees, makes any warranty, express or implied, or assumes any legal responsibility for the accuracy, completeness, or usefulness of any information, apparatus, product, or process disclosed, or represents that its use would not infringe privately owned rights. Reference herein to any specific commercial product, process, or service by its trade name, trademark, manufacturer, or otherwise, does not necessarily constitute or imply its endorsement, recommendation, or favoring by the United States Government or any agency thereof, or the Regents of the University of California. The views and opinions of authors expressed herein do not necessarily state or reflect those of the United States Government or any agency thereof or the Regents of the University of California.

LBL-16806

THERMODYNAMIC FRAMEWORK FOR ESTIMATING THE EFFICIENCIES OF ALKALINE BATTERIES

Final Report
October 1983

by
B. Pound, B. Sundararaj, R.P. Singh, and D.D. Macdonald
of
The Ohio State University

for

Technology Base Research Project
Lawrence Berkeley Laboratory
University of California
Berkeley, California 94720

This work was supported by the Assistant Secretary for Conservation and Renewable Energy, Office of Energy Systems Research, Energy Storage Division of the U.S. Department of Energy under Contract No. DE-AC03-76SF00098, subcontract no. 4505110 with the Lawrence Berkeley Laboratory.

ABSTRACT

A thermodynamic framework was developed to evaluate the efficiencies of alkaline battery systems for electrolyte concentrations from 1 to 8 mol kg^{-1} and over the temperature range -10 to 120°C. An analysis of the thermodynamic properties of concentrated LiOH, NaOH, and KOH solutions was carried out to provide data for the activity of water, the activity coefficient of the hydroxide ion, and the pH of the electrolyte. Potential-pH relations were derived for various equilibrium phenomena for the metals Li, Al, Fe, Ni, and Zn in aqueous solutions, and using the thermodynamic data for the alkali metal hydroxides, equilibrium potentials were computed as a function of composition and temperature. These data have then been used to calculate reversible cell potentials for a number of battery systems, assuming a knowledge of the cell reactions. The calculated reversible cell voltages are then compared with observed cell voltages to compute voltage efficiencies for various alkaline batteries.

The cell voltages varied with concentration of alkali metal hydroxide and temperature in a manner depending on the particular battery. In the case of the Al/air, Zn/air, and Zn/Ni systems, the cell voltage increased with concentration but decreased with an increase in temperature. In contrast, the Li/air and, to a lesser extent, the Fe/air cells exhibited the opposite behavior, while the cell potentials of the Fe/Ni system decrease with an increase in either concentration or temperature. The potential of the H_2/Ni cell, however, is independent of concentration but does decrease with temperature.

The efficiencies of H_2/Ni, Fe/Ni, and Zn/Ni test cells were found to be between 90-100%, implying that, at least at open circuit, there is little, if any, contribution from parasitic redox couples to the cell potentials for these systems. The efficiency of an Fe/air test cell was relatively low (72%), but this may be determined by the nature of the redox couple at the air electrode.

CONTENTS

	Page
INTRODUCTION	1
THERMODYNAMICS OF CONCENTRATED ALKALI HYDROXIDE SOLUTIONS	3
EXPERIMENTAL DETERMINATION OF VAPOR PRESSURE DATA FOR LiOH	8
Experimental for 0-60°C Data	9
System	9
Procedure	9
Experimental For Boiling Point Data	13
System	13
Procedure	15
PROPERTIES OF CONCENTRATED ALKALI HYDROXIDE SOLUTIONS	16
THERMODYNAMICS OF METALS IN CONCENTRATED ALKALI SOLUTIONS	23
Evaluation of Free Energy Functions	26
Equilibrium Potential/Concentration Data	27
THERMODYNAMICS OF ALKALINE BATTERIES	45
Cell Potentials	45
Efficiences	54
Uncertainties of Data Base	58
CONCLUSIONS	60
ACKNOWLEDGMENTS	60
REFERENCES	60

APPENDICES Page

A POLYNOMIAL COEFICIENTS FOR BEST FIT OF p/p° VS CONCENTRATION FOR LITHIUM HYDROXIDE A-1

POLYNOMIAL COEFICIENTS FOR BEST FIT OF p/p° VS CONCENTRATION FOR SODIUM HYDROXIDE A-2

POLYNOMIAL COEFICIENTS FOR BEST FIT OF p/p° VS CONCENTRATION FOR POTASSIUM HYDROXIDE A-3

B BASIC PROGRAM (ACTIV) TO CALCULATE THERMODYNAMIC PROPERTIES OF CONCENTRATED ALKALI HYDROXIDE SOLUTIONS B-1

C BASIC PROGRAM (THERM) TO CALCULATE THERMODYNAMIC PROPERTIES OF METALS IN CONCENTRATED ALKALI HYDROXIDE SOLUTIONS C-1

D FORTRAN PROGRAM (THERM) TO CALCULATE THERMODYNAMIC PROPERTIES OF METALS IN CONCENTRATED ALKALI HYDROXIDE SOLUTIONS D-1

E THERMODYNAMIC PROPERTIES OF LITHIUM, ALUMINUM, ZINC, NICKEL, IRON ANS OXYGEN IN CONCENTRATED ALKALI HYDROXIDE SOLUTIONS AS A FUNCTION OF TEMPERATURE E-1

ILLUSTRATIONS

Figure		Page
1.	Apparatus for vapor pressure determination.	10
2.	Cell connections to differential pressure transducer and to vacuum line.	11
3.	Apparatus for boiling point determination.	14
4.	Variation of the activity of water with concentration of LiOH, NaOH, KOH solutions as a function of temperature.	21
5.	Variation of the mean molal activity coefficients with concentration in concentrated solutions of LiOH, NaOH, and KOH as a function of temperature.	22
6.	Variation of pH with concentration for KOH, NaOH, and LiOH solutions as a function of temperature.	24
7.	Potential versus log m_{LiOH} diagrams for lithium in concentrated lithium hydroxide solution as a function of temperature.	30
8.	Potential versus log m_{NaOH} diagrams for lithium in concentrated sodium hydroxide solution as a function of temperature.	31
9.	Potential versus log m_{KOH} diagrams for lithium in concentrated potassium hydroxide solution as a function of temperature.	32

Figure		Page
10.	Potential versus log m_{LiOH} diagrams for aluminum in concentrated lithium hydroxide solution as a function of temperature.	33
11.	Potential versus log m_{NaOH} diagrams for aluminum in concentrated sodium hydroxide solution as a function of temperature.	34
12.	Potential versus log m_{KOH} diagrams for aluminum in concentrated potassium hydroxide solution as a function of temperature.	35
13.	Potential versus log m_{LiOH} diagrams for zinc in concentrated lithium hydroxide solution as a function of temperature.	36
14.	Potential versus log m_{NaOH} diagrams for zinc in concentrated sodium hydroxide solution as a function of temperature.	37
15.	Potential versus log m_{KOH} diagrams for zinc in concentrated potassium hydroxide solution as a function of temperature.	38
16.	Potential versus log m_{LiOH} diagrams for nickel in concentrated lithium hydroxide solution.	39
17.	Potential versus log m_{NaOH} diagrams for nickel in concentrated sodium hydroxide solution as a function of temperature.	40
18.	Potential versus log m_{KOH} diagrams for nickel in concentrated potassium hydroxide solution as a function of temperature.	41

Figure		Page
19.	Potential versus log m_{LiOH} diagrams for iron in concentrated lithium hydroxide solution as a function of temperature.	42
20.	Potential versus log m_{NaOH} diagrams for iron in concentrated sodium hydroxide solution as a function of temperature.	43
21.	Potential versus log m_{KOH} diagrams for iron in concentrated potassium hydroxide solution as a function of temperature.	44

TABLES

Table		Page
1.	The Effect of the Number of Integration Increments on the Values of Log $\gamma_{\pm}$ for NaOH.	6
2.	Vapor Pressure of Lithium Hydroxide and Activity of Water as a Function of Lithium Hydroxide Concentration and Temperature.	17
3.	Activity of Water for Alkali Hydroxide Solutions as a Function of Concentration and Temperature.	18
4.	Mean Molal Activity Coeficients for Alkali Hydroxide Solutions as a Function of Concentration and Temperature.	19
5.	pH for Alkali Hydroxide Solutions as a Function of Concentration and Temperature.	20
6.	Thermodynamic Data for Species Not Listed in References (10), (19), and (20).	28
7.	Equilbrium Potentials For Li/Air Cell in Concentrated Alkali Hydroxide Solutions.	46
8.	Equilibrium Potentials for Al/Air Cell in Concentrated Alkali Hydroxide Solutions.	47
9.	Equilibrium Potentials for Zn/Air Cell in Concentrated Alkali Hydroxide Solutions.	48

Table		Page
10.	Equilbrium Potentials for Fe/Air Cell in Concentrated Alkali Hydroxide Solutions.	49
11.	Equilibrium Potentials for Zn/Ni Cell in Concentrated Alkali Hydroxide Solutions.	50
12.	Equilibrium Potentials for Fe/Ni Cell in Concentrated Alkali Hydroxide Solutions.	51
13.	Equilibrium Potentials for H_2/Ni Cell in Concentrated Alkali Hydroxide Solutions (Discharged Condition).	52
14.	Equilibrium Potentials for H_2/Ni Cell in Concentrated Alkali Hydroxide Solutions (Charged Condition).	53
15.	Voltage Efficiences of Practical Battery Systems at Open Circuit.	56
16.	Comparison of Open Circuit Electrode Potentials, E_{oc} with Equilibrium Potentials, E.	57

INTRODUCTION

High energy alkaline batteries are being considered for vehicular propulsion and standby power source applications. Leading candidate battery systems for these applications include zinc-nickel, iron-nickel, hydrogen-nickel, zinc-air, iron-air, lithium-air, and aluminum-air. Some of these systems, e.g. iron-nickel and H_2/Ni, have already undergone substantial development, whereas others, e.g. aluminum- air, are in a research stage. The rational choice of the most suitable battery will involve a compromise between various characteristics that define the performance of the system; cost, energy, power, and conversion efficiency on both charging and discharging. This latter parameter is particularly important in the case of vehicular propulsion, since the battery will be subjected to extensive deep cycling and will have to compete with the more traditional fossil-fueled systems.

The complete analysis of the efficiency of an electrochemical energy storage or conversion system requires a knowledge of the thermodynamic properties of the cell reactions. Thus, the overall and thermal efficiences of the device may be defined, respectively, as:

$$\varepsilon = \left[- \int_{\alpha=0}^{\alpha=q} E \, d\alpha \right] / \Delta G \qquad (1)$$

$$\varepsilon_T = \left[- \int_{\alpha=0}^{\alpha=q} E \, d\alpha \right] / \Delta H \qquad (2)$$

where ΔG is the molar Gibbs ("Free") energy change, ΔH is the molar enthalpy change, α is the charge transferred through the external circuit, and E is the cell voltage. The symbol q is the total charge passed through the external circuit per mole of cell reaction; q may be less than or equal to nF where n is the stoichemetric number of electrons involved in the cell reaction and F is the Faraday (96487 C equiv^{-1}). A value for q of less than nF can arise from internal "chemical shorting" due to diffusion of anodic dissolution

products (e.g. $Zn(OH)_4^{2-}$, FeO_2^{2-}) to the cathode and from transport of cathodic products to the anode.

The voltage efficiency of the cell and the coulombic efficiency of a half cell reaction are defined as:

$$\varepsilon_V = E/E_{cell} \tag{3}$$

and

$$\varepsilon_C = q/nF \tag{4}$$

respectively, where E_{cell} is the reversible potential for the cell.

Evaluation of the efficiency of any given battery requires the experimental determination of q and E during both charging and discharging, a knowledge of the reactions taking place in the system (yields n), and an analysis of the thermodynamics of the cell to yield ΔG, ΔH, and E_{cell}. Note that E_{cell} is often equated to the "open circuit potential"; this is valid only in the absence of any internal shorting phenomena.

Assuming that the cell reactions are well defined, the change in Gibbs energy and enthalpy for the system and the reversible potential may be evaluated as follows:

$$\Delta G = \Sigma_{products}\ \nu_p\ \mu_p - \Sigma_{reactants}\ \nu_R\ \mu_R \tag{5}$$

$$\Delta H = \Delta G - T\left(\frac{\partial \Delta G}{\partial T}\right) \tag{6}$$

$$E_{cell} = -\Delta G^\circ/nF \tag{7}$$

where ν is the stoichiometric coefficient for a reactant (subscript R) or product (P) in the reaction, μ is the chemical potential, and ΔG° is the change in <u>standard</u> Gibbs energy for the cell reaction. The chemical potential can be further expanded to yield

$$\mu_i = \mu_i^\circ + RT\ln m_i + RT\ln\gamma_i \tag{8}$$

where μ_i° is the standard-state chemical potential of species i, m_i is the molal concentration, and γ_i is the activity coefficient. The evaluation of the thermodynamic quantities ΔG and ΔH involves not only a consideration of the reactants and products in their standard states, but also a knowledge of the activity coefficients of dissolved ions and activity of the solvent in the concentrated electrolyte solutions of interest (water is involved in many reactions). Because the efficiency of an electrochemical energy storage system is expected to vary with temperature, it is also desirable to evaluate the thermodynamic parameters over a wide range of environmental conditions.

Extensive thermodynamic data of the kind required are available for dilute systems over a wide range of temperaure. However, few data have been generated for the metals of interest (Fe, Ni, Zn, Al, and Li) in concentrated alkali solution (1-15 mol kg^{-1}) over the temperature range (-20 to 150°C) that is expected for some applications. This report describes a study which has been carried out to assess the thermodynamic properties of the metals of interest in concentrated LiOH, NaOH, and KOH media as a function of composition and temperature. The thermodynamic data generated have been used to compute equilibrium potentials for a large number of reactions involving Fe, Ni, Zn, Al and Li in concentrated LiOH, NaOH and KOH solutions (1-8 mol kg^{-1}) at temperatures from -10 to 120°C. These data have then been used to calculate reversible cell potentials for a number of battery systems, assuming a knowledge of the cell reactions. The calculated reversible cell voltages are then compared with observed cell voltages to compute voltage efficiencies for various alkaline batteries.

THERMODYNAMICS OF CONCENTRATED ALKALI HYDROXIDE SOLUTIONS

Concentrated solutions of alkali metal hydroxides exhibit non-ideal behavior. The activity of the solvent, in this case water, cannot be assumed to be unity. In addition, the activity depends upon the identity of the cation (Li^+, Na^+, K^+), contrary to the behavior in dilute solutions. Furthermore, the activity of the alkali metal hydroxide varies with concentration and temperature in a non-ideal manner as short range interactions become significant when the mean distance between the solute particles is small (1,2). The activity coefficient of the hydroxide ion in solution is

also affected by the cation because of ion pair formation which increases along the series KOH<NaOH<LiOH (3-6).

If the vapor pressure is low enough that fugacity corrections can be ignored, the activity of water in solution can be found from Raoult's law as

$$a_w = p/p^\circ \tag{9}$$

where p and p° are the vapor pressures of the solution and pure water, respectively. The pressures are low enough up to 120°C that the error incurred by ignoring fugacity coefficient corrections have been estimated (7) to be no more than a few percent.

The osmotic coefficient for the medium, ϕ, is related to the activity of water by equation (10)

$$\phi = -1000 \ln a_w/M\nu m \tag{10}$$

where M is the molecular weight of H_2O (18.016), and ν is the number of ions into which the electrolyte dissociates in solution (ν=2 for the alkali metal hydroxides). According to the Gibbs-Duhem equation, the change in the stoichiometric mean molal activity coefficient of the solute with concentration is given by

$$d\ln\gamma_\pm = -(1/m)\ d[m(1-\phi)] \tag{11}$$

which on integration yields

$$\ln\gamma_\pm = -(1-\phi) - 2\int_0^m \left(\frac{1-\phi}{m}\right) d\sqrt{m} \tag{12}$$

Evaluation of the integral in equation (12) therefore allows the activity coefficient $\gamma_\pm$ to be determined.

The observed uncertainty in the osmotic coefficient at low concentrations increases sharply as m is decreased. Consequently, the variation of $1-\phi$ with

m is more satisfactorily described by using Debye-Huckel theory(6), which predicts that for low concentrations

$$(1-\phi)/\sqrt{m} = 0.7676\ A\sqrt{d_o}\cdot\sigma_m \tag{13}$$

where d_o is the density of the solvent and

$$\sigma_m = \sum_{n=1}^{\infty} \left(\frac{3n}{n+2}\right) \left(-A'_m\sqrt{m}\right)^{n-1} \tag{14}$$

The Debye-Huckel coefficients are given by

$$A = 1.814 \times 10^6/(DT)^{3/2} \tag{15}$$

and

$$A'_m = 153/\sqrt{DT} \tag{16}$$

where D is the dielectric constant of water at the temperature of interest. The data of Akerlof and Oshry (8) for D as a function of temperature were used for the evaluation of A and A'_m.

Previous work(7) has shown that the upper concentration limit for equation (13) is 0.8 mol kg^{-1}. Hence, $(1-\phi)/\sqrt{m}$ can be calculated over the low concentration range (0 to 0.8 mol kg^{-1}) using equation (13), but for higher concentrations this function must be evaluated from experiment using equation (10).

In this study, $\ln\gamma_\pm$ was calculated from equation (12) by an iterative technique using the trapezoidal rule to evaluate the integral. The $\sqrt{m}$ field was divided into 80, 160, 320, 640, 800 and 1600 increments to determine the minimum number required to achieve an acceptable level of precision. The effect of varying the number of integration increments on the values of $\log \gamma_\pm$ calculated using equation (12) for NaOH is shown in Table 1. In all cases, $\log \gamma_\pm$ becomes more positive as the increments are made smaller. However, there is little change in $\log\gamma_\pm$ as N is increased from 320 to 1600 increments, and therefore the values given by N = 1600 are regarded as sufficiently precise for subsequent pH calculations.

TABLE 1

THE EFFECT OF THE NUMBER OF INTEGRATION INCREMENTS ON THE VALUES OF LOG $\gamma_{\pm}$ FOR NaOH.

T/K	m/mol kg^{-1}	Log $\gamma_{\pm}$ Number of Increments, N					
		80	160	320	640	800	1600
	1	-0.171	-0.167	-0.165	-0.164	-0.164	-0.164
298	4	-0.104	-0.100	-0.098	-0.097	-0.097	-0.096
	8	0.225	0.229	0.231	0.232	0.232	0.233
	1	-0.266	-0.263	-0.261	-0.261	-0.261	-0.260
393	4	-0.256	-0.253	-0.252	-0.251	-0.251	-0.251
	8	-0.129	-0.126	-0.125	-0.124	-0.124	-0.124

The definition of pH as -log a_{H^+} was retained for the concentrated hydroxide systems treated in this study with the understanding that it is a purely formal relationship requiring a_{H^+} itself to be specified. In the absence of more reliable data for quantities such as $\gamma_{\pm}$, this definition is considered to provide an adequate estimate of the pH.

On this basis, the pH of concentrated hydroxide solutions could be calculated using either the ionic product of water (Q_w) or the dissociation constant (K_w) of water. However, values of Q_w reported in the literature were derived from experimental studies with KCl solutions and furthermore are strictly valid only for concentrations less than 3.0 mol kg^{-1}. It would therefore be necessary to assume that the same values of Q_w hold for concentrated hydroxide solutions.

In order to avoid this assumption, it was decided to use in this analysis the dissociation constant which is given by

$$K_w = \frac{a_{H^+} a_{OH^-}}{a_w} \qquad (17)$$

An expression for K_w as a function of temperature is given by Naumov et al (10). Introduction of K_w and rearrangement leads to the following equation for the pH

$$pH = \log \frac{m_{OH^-} \gamma_{\pm}^*}{a_w} + \frac{4466.2}{T} - 5.941 + 0.016638T \qquad (18)$$

where $\gamma_{\pm}^*$ is the mean ionic activity coefficient and m_{OH^-} is the concentration of free hydroxide ions. In concentrated solutions, however, it is the stoichiometric concentration, m_{MOH}, of alkali metal hydroxide that is experimentally the most convenient variable, but this quantity differs from m_{OH^-} due to ion pairing:

$$m_{MOH} = m_{OH^-} + m_{comp} \qquad (19)$$

where m_{comp} is the concentration of ion pairs. Although the value of the product $m_{OH^-} \gamma_{\pm}^*$ is not known, it may be obtained by application of the following relationship (11):

$$m_{OH^-} \gamma_{\pm}^* = m_{MOH} \gamma_{\pm} \qquad (20)$$

The pH equation can now be expressed as

$$pH = \log \frac{m_{MOH} \gamma_{\pm}}{a_w} + \frac{4466.2}{T} - 5.941 + 0.016638T \qquad (21)$$

Clearly, in order to evaluate the pH, as well as $\gamma_{\pm}$ from equation (12), the activity of water must be known at the appropriate concentration of each hydroxide solution. Sufficient data are available in the literature for the vapor pressure of NaOH and KOH solutions over the desired concentration and temperature ranges, thereby allowing values of a_w to be obtained using equation (9). Vapor pressure data for KOH were taken from the work of Anisimov (12), and of Bro and Kang (13), while those for NaOH were calculated using the following equation derived by MacMullin (14):

$$\frac{p}{p_o} = 1 + [(T-174)\ (a + bm + cm^2 + d/m) - 0.03170]m \qquad (22)$$

where m is the molality of the solution, p° is the vapor pressure of pure water at temperature T (°C), and the coefficients a, b, c, and d have the following values

$$a = -8.6715 \times 10^{-5}$$
$$b = 3.368 \times 10^{-5}$$
$$c = -1.354 \times 10^{-6}$$
$$d = 7.88 \times 10^{-5}$$

Equation (22) is strictly valid for temperatures between 20 and 100°C but it is assumed that extrapolation to -10° and to 120°C can be made with negligible error. Equation (22) is also valid for $m < 12.5$ mol kg^{-1}, which therefore includes the solutions of interest in this work.

The vapor pressure data for both NaOH and KOH solutions were plotted against concentration for each temperature, and a smoothed set of data over the concentration range selected. A statistical analysis of this data was performed to obtain the most appropriate polynomials to describe the variation of the activity of water with concentration at each temperature. The calculations were performed using a SAS (Statistical Analysis of Systems) program and yielded values for the coefficients in equation (23).

$$\frac{p}{p^\circ} = \sum_{i=o}^{k} A(i)m^i \qquad (23)$$

Values for these coefficients are listed in Appendix A.

Insufficient vapor pressure data were available for LiOH to generate values of a_w. As a result, these data had to be obtained from an experimental study which is described in the following section.

EXPERIMENTAL DETERMINATION OF VAPOR PRESSURE DATA FOR LiOH

Adequate thermodynamic data were generated from literature sources (12-14) to compute water activities and ionic activity coefficients for concentrated NaOH and KOH solutions over the desired temperature range. However, a lack of data exists for LiOH solutions, particularly with regard to vapor pressures from which water activities can be calculated. An experimental program was therefore initiated to obtain vapor pressures of concentrated LiOH solutions

at various temperatures within the range of interest. Vapor pressure measurements were performed over the range 0 to 60°C using one experimental system and at the boiling point of each LiOH solution using a second system. Data for desired temperatures were then obtained by extrapolation and interpolation of the measured values of vapor pressure.

Experimental for 0-60°C Data

System.

The experimental cell and the associated apparatus are shown schematically in Figures 1 and 2, respectively. The cell consists of two Ni-200 tubes, each 15.2 cm long and 2.2 cm in diameter. The lower ends of the tubes are closed. Stainless-steel transfer lines extend from the top of each tube and are connected to the differential pressure transducer (Setra Systems, Model 228, Range 0-10 PSID, Accuracy ±0.25% FS) and to the vacuum system. The Ni tubes are contained within a polyethylene vessel 16.5 cm wide and 46 cm long, through which pre-thermostated glycol is circulated from a constant-temperature bath. The vessel is insulated by wrapping it with two layers of asbestos tape. A stirrer is located at the center of the vessel in order to ensure temperature uniformity, and a sensitive thermometer (±.02°C) is employed to measure the temperature of the tubes.

The vacuum system consists of a mechanical pump (Welch Duo Seal, 1/3 H.P. ultimate vacuum 0.05 mm of Hg), a diffusion pump (Speedivac, Model 1021, ultimate vacuum 10^{-5} torr), a liquid nitrogen trap, and a McLeod vacuum gauge. The vacuum lines are constructed from 9.5 cm I.D. Cu-Ni tubing. "Swagelok" standard vacuum valves and connectors are used in fabricating the apparatus.

Procedure.

Reagent grade LiOH was dissolved in double distilled carbon dioxide-free water. Carbon dioxide was removed from the water by boiling followed by cooling in airtight containers. The solutions were stored in polyethylene vessels. A small amount of barium hydroxide was added to the solution to remove the last traces of CO_2. The strength of each solution was determined by titrating against HCl of known concentration.

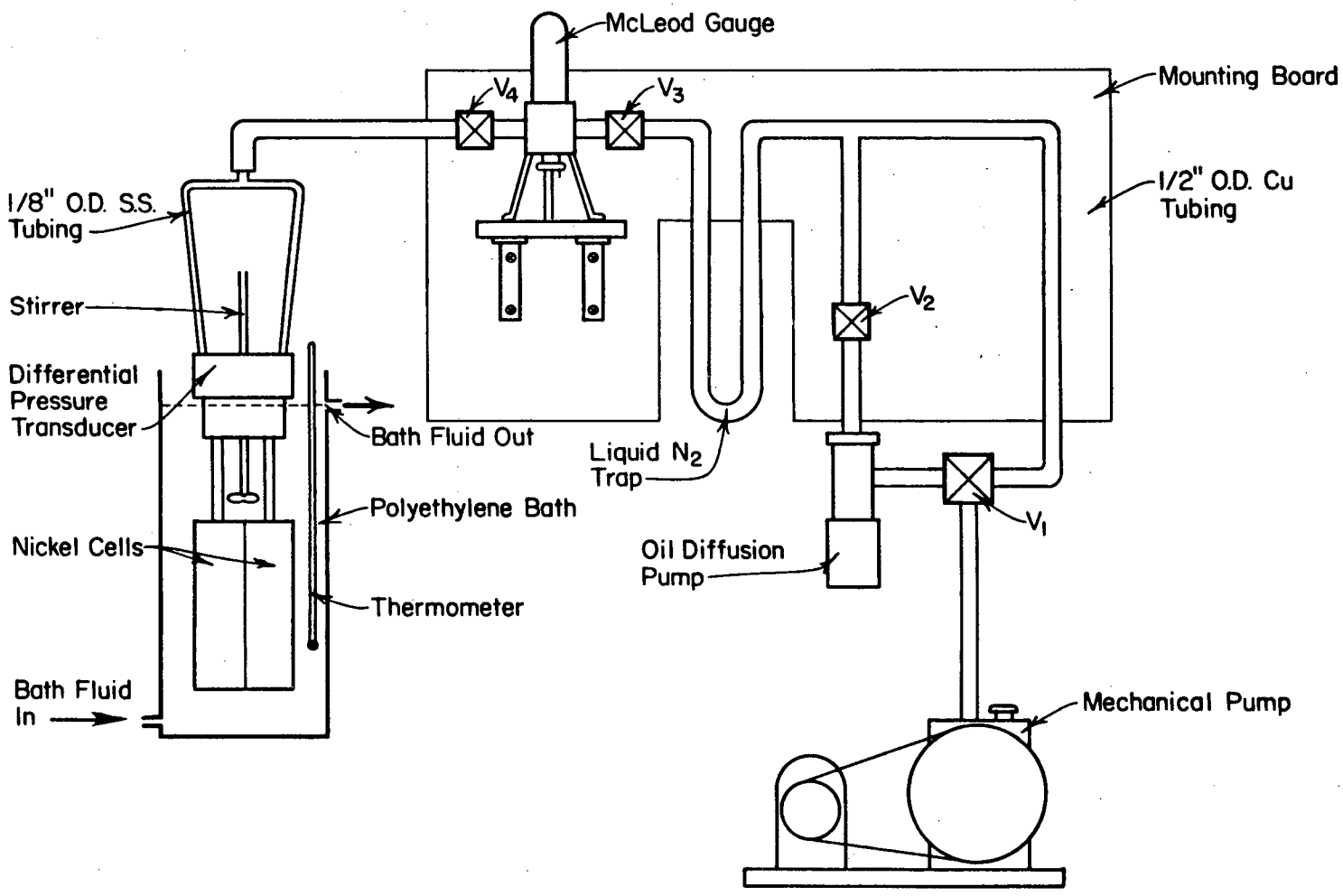

Figure 1. Apparatus for vapor pressure determination.

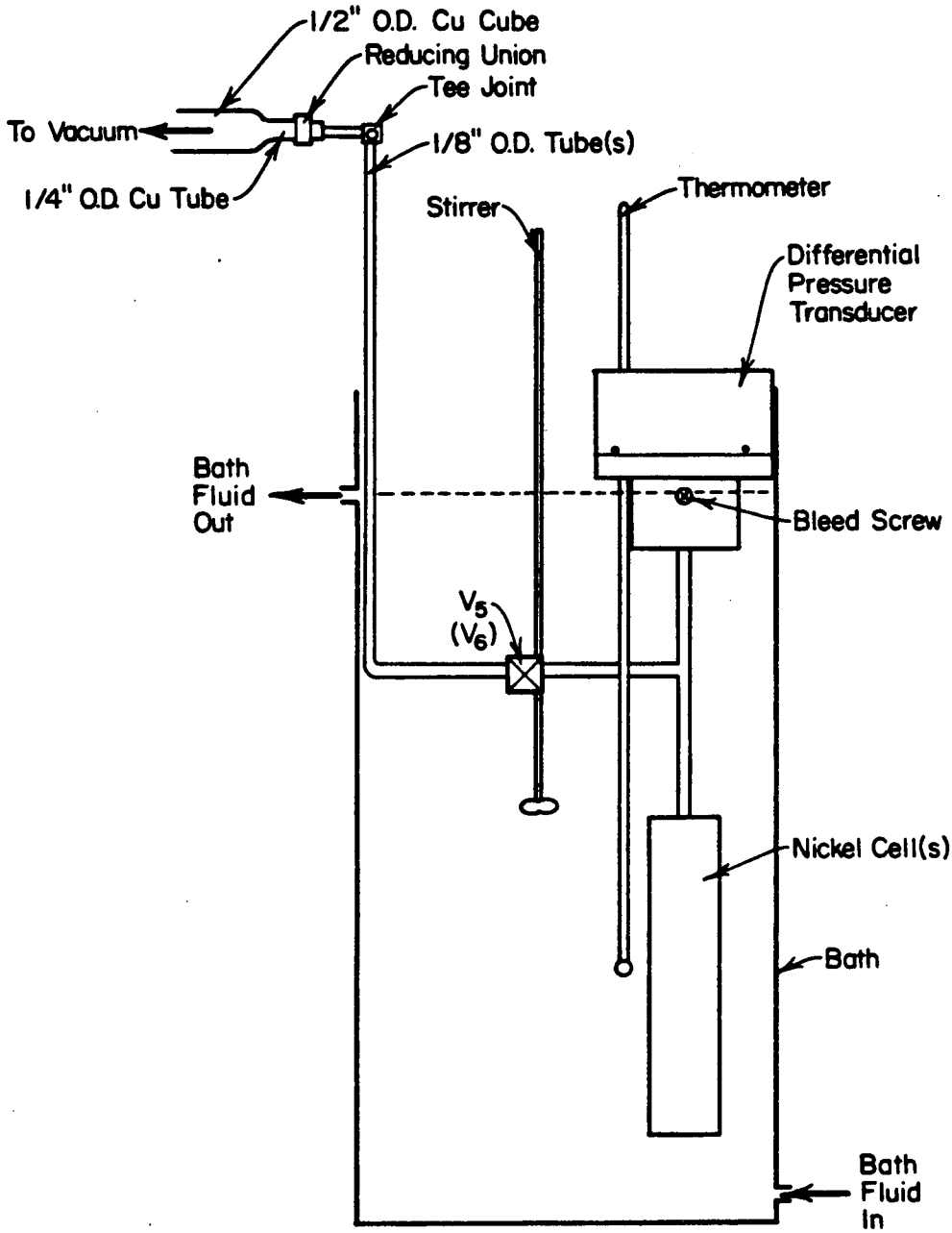

Figure 2. Cell connections to differential pressure transducer and to vacuum line.

To remove the residual gases from the solution the experimental cells were frozen and evacuated three times before each experiment. The whole system was evacuated to 0.03 torr using the mechanical pump keeping valve V_4 closed and valve V_1 connected to the vacuum line directly. Then valve V_1 was turned to connect the mechanical pump to the diffusion pump and valve V_2 was opened. In this position the mechanical pump acts as a back-up for the oil diffusion pump. When a vacuum of better than 10^{-2} torr was achieved, the Ni cells were connected to the vacuum line and to the differential pressure transducer (DPT). One cell contained 40 cc of double distilled water whereas the other contained 40 cc of the test solution of known concentration. Precautions were taken to ensure that all of the joints were air tight. The valves V_5 and V_6 were then opened to establish equal pressures in each port of the DPT. The cell was then immersed in a liquid N_2 container. The container was raised up slowly so that the cell solutions froze from the bottom unidirectionally. If this procedure were not followed, the thermal shock and sudden expansion of water would lead to distortion of the Ni cells. After the contents of the Ni cells were completely frozen, valve V_4 was opened and the whole system was evacuated to a pressure of less than 0.01 torr.

After evacuating the cells as outlined above, valves V_5 and V_6 were closed and the cells were immersed in warm water. Every ten minutes the water was siphoned off and replaced with fresh warm water. The process was continued until the contents of the Ni cells reached approximately 60°C. The Ni cells were then refrozen as described above. At this stage, the bleed screws were removed and compressed air was passed through the DPT ports to flush out any condensed liquid. The bleed screws were then closed in order to check the continuity of the stainless steel transfer lines, by opening valves V_5 and V_6 briefly to observe the suction in each port of the DPT. A good suction indicated that the transfer lines were clear. Blocking of transfer lines was observed frequently, especially at the joints above the Ni cells. In this situation, the liquid N_2 flask was removed temporarily and the stainless steel lines were warmed by passing compressed air over them. This melted the blocking material which subsequently moved into the Ni cells. This procedure of freezing, evacuating, and warming was repeated three times to ensure that the residual gases from the solutions had been removed.

After the freezing and evacuation process, the Ni cells were immersed in a thermostated glycol bath. To prevent condensation, the stainless-steel transfer line and most of the DPT were also immersed in the glycol bath. A uniform temperature was maintained throughout the bath by a stirrer which was located at the center of the bath. The temperature of the bath was measured using a thermometer (±0.02°C) placed very close to the Ni cells. The top of the bath was covered with thick pads of styrofoam to minimize heat loss.

The zero differential pressure, Δp_o, was measured at a temperature of approximately 0°C by keeping valves V_5 and V_6 open and valve V_4 closed. After a steady reading was obtained, valves V_5 and V_6 were closed. The bath temperature was then set at a different desired temperature and the corresponding readings for the depression in vapor pressure (Δp_{obs}) were obtained. The true value for Δp was obtained from the following relationship:

$$\Delta p = \Delta p_{obs} - \Delta p_o \tag{24}$$

The experimental technique was tested by measuring vapor pressures for NaOH solutions of known concentrations. The results obtained were in very good agreement (<1%) with values generated from the literature (14).

Experimental For Boiling Point Data

Vapor pressures could not be obtained at temperatures greater than 60°C using the experimental system just described due to the temperature limitations of the differential pressure transducer. In order to generate more reliable data by extrapolation and interpolation for the desired temperature range, a single vapor pressure datum was obtained at the boiling point of the LiOH solution for each concentration studied.

System

An experimental apparatus to determine the boiling point of each LiOH solution is shown schematically in Figure 3. It consists of a cylindrical nickel cell 14.0 cm long, 2.5 cm O.D. and 1.65 mm wall thickness. The top of the cell is open while the other end is fitted with a "Swagelok" male connector which in turn is connected to a 'Whitey' ball valve by a 3.18 mm O.D. stainless-steel tube. The other side of the valve is connected to a

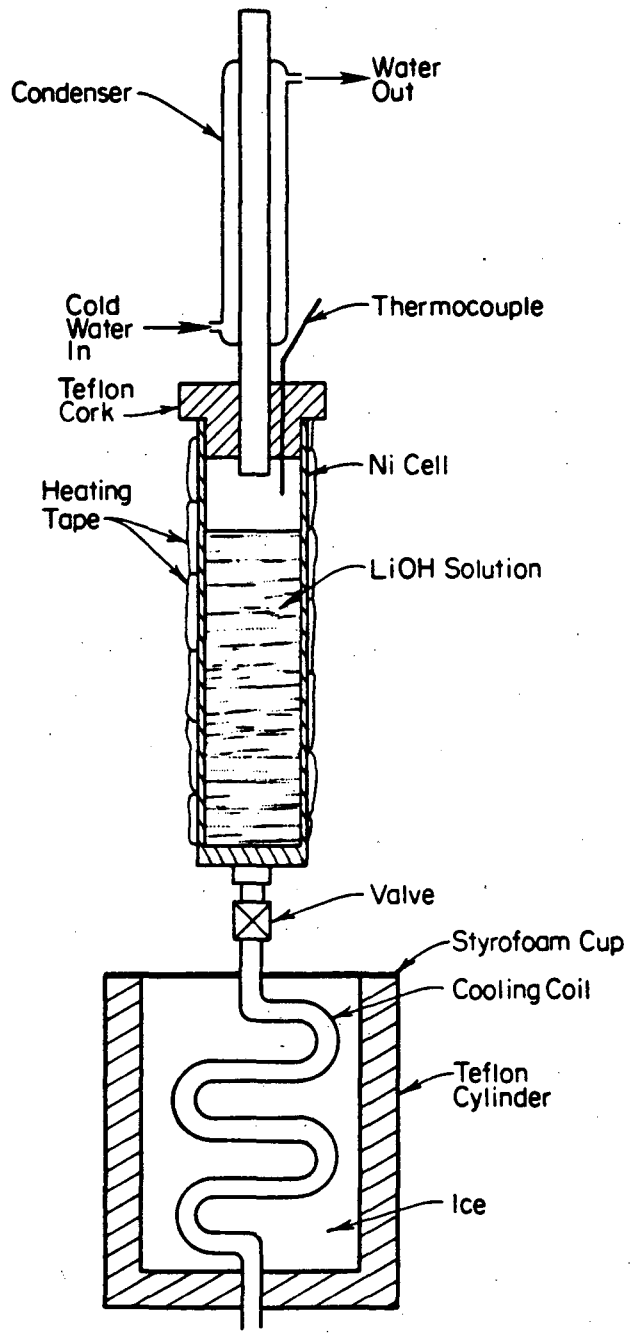

Figure 3. Apparatus for boiling point determination.

cooling coil made of 3.18 mm O.D. stainless steel tube, which passes through the bottom of the cylinder.

The top of the Ni cell is sealed with a Teflon cap which has a hole of 0.7 mm diameter at the center in order to accommodate a glass condenser through which cold water is circulated. A copper-constantan thermocouple which extends into the in cell by about 1.3 cm is also fitted through the Teflon cap. A heating tape connected to the power supply through a variac is wrapped around the Ni tube for controlled heating.

Procedure

Solutions were prepared as described in the preceeding experimental section. About 40 cc of the LiOH solution was placed in the Ni cell with the bottom valve closed. The Teflon cap was then fitted to the cell followed by the condenser and the thermocouple. The thermocouple was connected to a millivoltmeter through an ice junction in order to allow for the room temperature correction. The cell was heated at a rate of 2-3°C per minute, with the increase in temperature monitored by the thermocouple. The temperature at which the thermocouple reading became constant for 3-5 minutes was taken as the boiling point temperature of the solution.

The solution was then extracted slowly through the cooling coil by opening the valve at the bottom of the Ni cell and immediately titrating against a standard solution of HCl to determine the exact LiOH concentration. The experiment was repeated for the different concentrations of LiOH solutions studied.

The atmosphere pressure was measured using a barometer wtih an accuracy of 0.01 mm of Hg. The vapor pressure, p, of the solution was taken as the atmosphere pressure at the boiling point of the solution, and the vapor pressure depression, Δp, was calculated from equation (25)

$$\Delta p = p^{\circ} - p \tag{17}$$

where p° is the vapor pressure of water.

The combined low temperature (0-60°C) and boiling point data were plotted as a function of temperature and concentration. The Δp values for a given LiOH concentration at the desired temperatures were then obtained. The vapor pressure data for LiOH at various concentrations and temperatures are reported in Table 2. Also shown are the corresponding values of the water activity calculated from equation (9). As with NaOH and KOH, the LiOH data were subjected to a statistical analysis to provide values for the coefficients A(i) in equation (23). The resulting values for the coefficients are given in Appendix A.

PROPERTIES OF CONCENTRATED ALKALI HYDROXIDE SOLUTIONS

Values of a_w, log $\gamma_\pm$ and pH for concentrated LiOH, NaOH and KOH solutions were calculated using the program ACTIV given in Appendix B. These values are given in Tables 3 to 5, respectively, as a function of temperature and concentration. It should be noted that the program THERM (Appendix C) described in the following section also provides the values of a_w and pH.

The activity of water is shown in Figure 4 to decrease markedly as the stoichiometric concentration increases, with the effect being most pronounced at the lowest temperature. In contrast, the value of a_w generally increases with temperature although in the case of KOH solutions, a_w, initially passes through a maximum at 273K (see Table 3).

Log $\gamma_\pm$ is plotted against $\sqrt{m}$, as shown in Figure 5, in order to provide a comparison with previous studies. The data for LiOH at 298K are in excellent agreement with those quoted by Harned and Owen (6). In the case of NaOH, there is still reasonable agreement between the calculated and literature (6, 29) data at 298K whereas the corresponding data for KOH exhibit a significant difference at concentrations above 1 mol kg^{-1}. In view of the better agreement for LiOH and NaOH for which non-ideal behavior is expected to be more pronounced, the analysis to obtain log $\gamma_\pm$ appears to be adequate. However, in the case of KOH, it is possible that considerable error may exist in the water activity data used in the calculations, as suggested by the surprisingly linear dependence of a_w on concentration up to 8 mol kg^{-1}.

TABLE 2

VAPOR PRESSURE OF LITHIUM HYDROXIDE AND ACTIVITY OF WATER AS A FUNCTION OF LITHIUM HYDROXIDE CONCENTRATION AND TEMPERATURE

Conc. Molal	0°C		10°C		20°C		30°C		40°C		50°C		60°C	
	Vapor Pressure Torr	a_w	Vapor Pressure Torr	a_w	Vapor Pressure Torr	a_w	Vapor Pressure Torr	a_w	Vapor Pressure Torr	a_w	Vapor Pressure Torr	a_w	Vapor Pressure Torr	a_w
0.51	4.424	0.966150	8.904	0.966880	16.9675	0.967636	30.789	0.967477	53.564	0.961787	80.57	0.968220	144.7175	0.968788
1.08	4.329	0.945403	8.739	0.948963	16.6400	0.948590	30.194	0.948781	52.504	0.949028	87.78	0.948870	141.8500	0.949592
2.10	4.169	0.910461	8.429	0.915300	15.955	0.912175	29.044	0.912645	50.504	0.912877	84.54	0.913847	136.8000	0.915785
4.16	3.779	0.825289	7.649	0.830600	14.585	0.831754	26.534	0.833773	46.224	0.835514	77.31	0.835693	125.4400	0.839738
4.95	3.529	0.770692	7.109	0.771960	13.585	0.774740	24.774	0.778470	43.224	0.78129	72.71	0.78597	117.9800	0.789800

Conc. Molal	70°C		80°C		90°C		100°C		110°C		120°C			
	Vapor Pressure Torr	a_w	Vapor Pressure Torr	a_w	Vapor Pressure Torr	a_w	Vapor Pressure Torr	a_w	Vapor Pressure Torr	a_w	Vapor Pressure Torr	a_w	Vapor Pressure Torr	a_w
0.51	226.65	0.96983	344.25	0.96944	509.36	0.96881	736.70	0.96934	1043.76	0.97134	1149.14	0.97314		
1.08	224.40	0.95165	338.40	0.95297	502.46	0.95568	729.05	0.95928	1034.86	0.96306	1439.84	0.96689		
2.10	214.70	0.91869	325.60	0.91693	481.96	0.91669	698.90	0.91961	993.56	0.92462	1386.54	0.93110		
2.98	204.20	0.87377	311.10	0.87609	460.81	0.87647	668.60	0.87974	949.56	0.88367	1326.84	0.89101		
4.16	197.40	0.84467	300.35	0.84582	443.46	0.84347	642.40	0.84526	917.16	0.85352	1283.84	0.86214		
4.95	185.50	0.79375	282.70	0.79611	421.36	0.80143	610.00	0.80263	878.16	0.81723	1243.69	0.83578		

TABLE 3

ACTIVITY OF WATER FOR ALKALI HYDROXIDE SOLUTIONS
AS A FUNCTION OF CONCENTRATION AND TEMPERATURE

m/mol kg^{-1}	a_w Temperature/K							
	263	273	298	313	333	353	373	393
LiOH								
1	0.962	0.969	0.970	0.970	0.971	0.972	0.972	0.972
2	0.931	0.937	0.939	0.940	0.942	0.943	0.943	0.944
3	0.900	0.905	0.908	0.910	0.912	0.915	0.914	0.917
4	0.869	0.874	0.877	0.880	0.883	0.886	0.885	0.890
5	0.838	0.842	0.846	0.850	0.854	0.858	0.856	0.865
NaOH								
1	0.963	0.965	0.964	0.966	0.966	0.966	0.967	0.967
2	0.930	0.932	0.932	0.933	0.933	0.934	0.934	0.935
3	0.888	0.890	0.892	0.893	0.895	0.897	0.898	0.900
4	0.839	0.841	0.846	0.848	0.851	0.855	0.859	0.863
5	0.783	0.786	0.794	0.798	0.803	0.811	0.817	0.824
6	0.721	0.726	0.739	0.744	0.751	0.764	0.773	0.784
7	0.657	0.664	0.680	0.688	0.698	0.715	0.727	0.742
8	0.590	0.600	0.620	0.630	0.643	0.665	0.680	0.701
KOH								
1	0.924	0.969	0.961	0.962	0.966	0.965	0.964	0.963
2	0.865	0.911	0.903	0.908	0.912	0.912	0.913	0.913
3	0.807	0.853	0.845	0.853	0.857	0.860	0.862	0.864
4	0.748	0.795	0.787	0.799	0.803	0.807	0.811	0.815
5	0.689	0.738	0.729	0.744	0.749	0.755	0.760	0.766
6	0.631	0.680	0.671	0.690	0.695	0.702	0.709	0.717
7	0.572	0.622	0.613	0.635	0.641	0.650	0.658	0.667
8	0.514	0.564	0.555	0.581	0.587	0.597	0.607	0.618

TABLE 4

MEAN MOLAL ACTIVITY COEFFICIENTS FOR ALKALI HYDROXIDE SOLUTIONS AS A FUNCTION OF CONCENTRATION AND TEMPERATURE

m/mol kg^{-1}	log $\gamma_{\pm}$ Temperature/K							
	263	273	298	313	333	353	373	393
LiOH								
1	-0.129	-0.241	-0.266	-0.275	-0.287	-0.307	-0.329	-0.340
2	-0.158	-0.264	-0.297	-0.314	-0.334	-0.361	-0.377	-0.393
3	-0.170	-0.272	-0.310	-0.331	-0.357	-0.387	-0.400	-0.426
4	-0.174	-0.273	-0.315	-0.339	-0.370	-0.403	-0.413	-0.449
5	-0.174	-0.270	-0.315	-0.342	-0.376	-0.412	-0.421	-0.468
NaOH								
1	-0.144	-0.179	-0.164	-0.203	-0.220	-0.230	-0.244	-0.260
2	-0.164	-0.191	-0.190	-0.217	-0.235	-0.247	-0.263	-0.280
3	-0.117	-0.144	-0.155	-0.182	-0.205	-0.225	-0.247	-0.271
4	-0.043	-0.073	-0.096	-0.127	-0.156	-0.187	-0.217	-0.251
5	0.046	0.011	-0.025	-0.061	-0.097	-0.141	-0.179	-0.224
6	0.145	0.103	0.056	0.012	-0.031	-0.089	-0.136	-0.193
7	0.252	0.203	0.142	0.091	0.039	-0.034	-0.090	-0.159
8	0.365	0.307	0.233	0.173	0.112	0.024	-0.042	-0.124
KOH								
1	0.470	-0.245	-0.130	-0.159	-0.216	-0.207	-0.208	-0.196
2	0.714	-0.034	0.087	0.026	-0.037	-0.042	-0.057	-0.060
3	0.879	0.109	0.235	0.152	0.085	0.071	0.047	0.034
4	1.015	0.227	0.356	0.255	0.185	0.164	0.133	0.113
5	1.137	0.333	0.465	0.348	0.275	0.248	0.210	0.183
6	1.253	0.433	0.568	0.436	0.360	0.327	0.283	0.250
7	1.367	0.530	0.669	0.522	0.444	0.404	0.355	0.315
8	1.482	0.629	0.771	0.608	0.527	0.482	0.426	0.380

TABLE 5

pH FOR ALKALI HYDROXIDE SOLUTIONS AS A FUNCTION OF CONCENTRATION AND TEMPERATURE

m/mol kg^{-1}	pH Temperature/K							
	263	273	298	313	333	353	373	393
LiOH								
1	15.30	14.73	13.75	13.27	12.74	12.29	11.93	11.64
2	15.59	15.02	14.03	13.55	13.01	12.55	12.19	11.90
3	15.77	15.21	14.21	13.72	13.17	12.72	12.36	12.06
4	15.90	15.35	14.35	13.85	13.30	12.84	12.49	12.17
5	16.02	15.46	14.46	13.96	13.40	12.94	12.59	12.26
NaOH								
1	15.29	14.80	13.86	13.35	12.81	12.37	12.01	11.72
2	15.58	15.10	14.15	13.65	13.11	12.67	12.31	12.02
3	15.83	15.34	14.38	13.88	13.33	12.89	12.52	12.22
4	16.05	15.56	14.58	14.08	13.53	13.07	12.69	12.38
5	16.27	15.77	14.78	14.27	13.71	13.24	12.85	12.53
6	16.48	15.98	14.97	14.45	13.88	13.39	13.00	12.66
7	16.69	16.18	15.16	14.63	14.05	13.54	13.14	12.78
8	16.91	16.39	15.35	14.81	14.22	13.69	13.27	12.90
KOH								
1	15.92	14.73	13.89	13.39	12.81	12.40	12.05	11.79
2	16.49	15.27	14.44	13.90	13.32	12.89	12.53	12.25
3	16.86	15.61	14.79	14.23	13.64	13.20	12.83	12.54
4	17.16	15.88	15.07	14.49	13.89	13.45	13.07	12.77
5	17.41	16.12	15.31	14.71	14.11	13.66	13.27	12.97
6	17.65	16.34	15.52	14.91	14.31	13.85	13.45	13.14
7	17.87	16.54	15.73	15.10	14.49	14.02	13.62	13.30
8	18.09	16.74	15.93	15.28	14.67	14.20	13.79	13.46

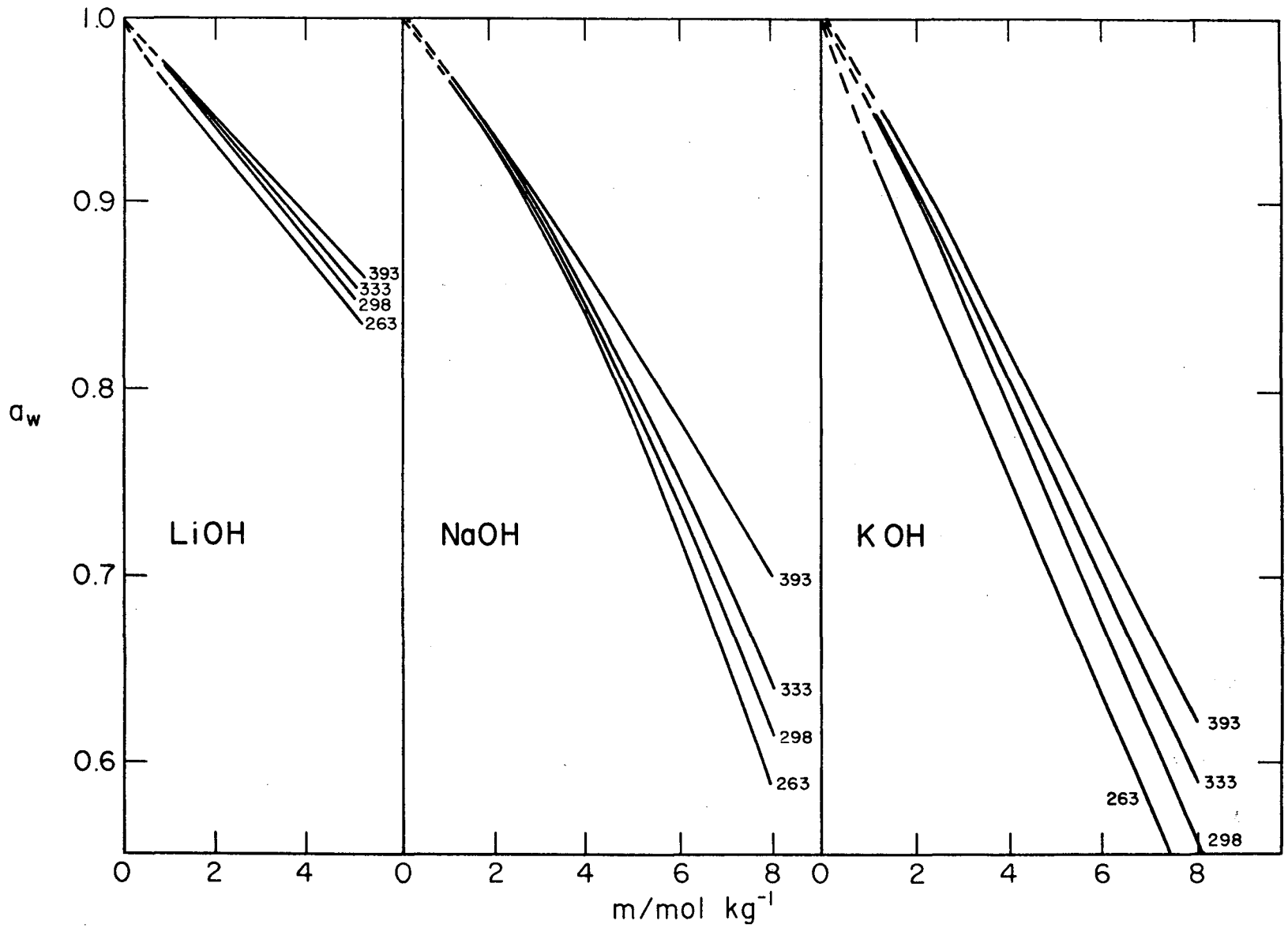

Figure 4. Variation of the activity of water with concentration of LiOH, NaOH, and KOH solutions as a function of temperature.

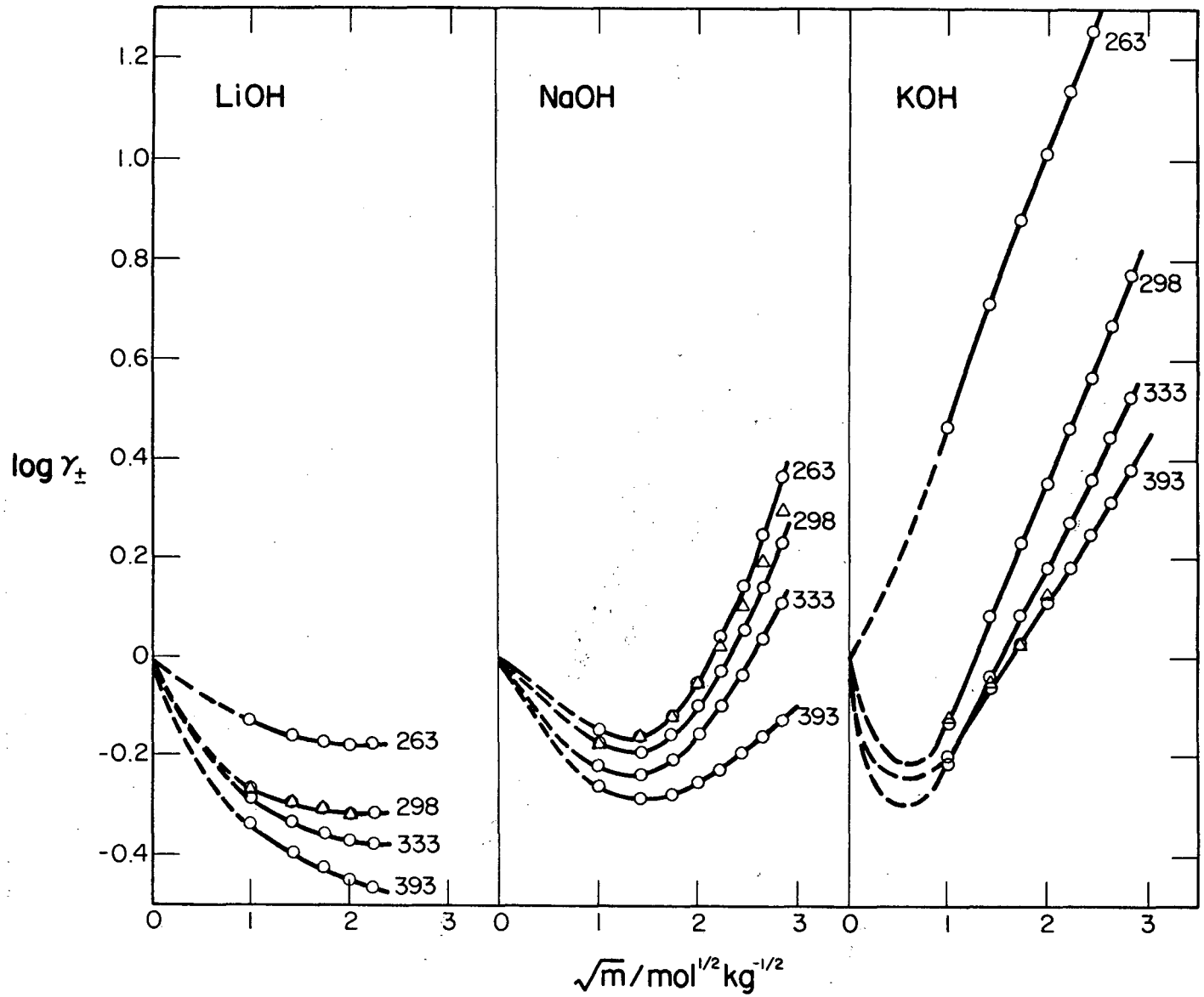

Figure 5. Variation of the mean molal activity coefficients with concentration in concentrated solutions of LiOH, NaOH, and KOH as a function of temperature. The symbol, Δ, represents literature data (6, 29) at 298 K.

In general, log $\gamma_{\pm}$ decreases with increasing temperature, but NaOH ($m \leq 2$ mol kg^{-1}) and KOH solutions initially exhibit a minimum (in this case at 273 K.) The dependence of log $\gamma_{\pm}$ on concentration varies with the cation; LiOH solutions display a decrease wth increasing concentration over the range shown whereas NaOH exhibits a minimum followed by a marked increase in log $\gamma_{\pm}$. Similarly, the data for KOH increases subsequent to an apparent minimum as observed in earlier work (28).

The pH of concentrated hydroxide solutions is shown in Figure 6 to vary non-linearly with composition but it nevertheless exhibits a steady increase over the range of molalities shown. The increase in pH with composition is similar for both NaOH and KOH but the effect is less marked for LiOH. It is also apparent that the pH decreases along the series KOH > NaOH > LiOH for any given stoichiometric concentration. This decrease reflects a corresponding increase in ion pairing for the alkali hydroxides in solution.

THERMODYNAMICS OF METALS IN CONCENTRATED ALKALI SOLUTIONS

The thermodynamic properties of metals in aqueous media can be derived for reactions having the general form

$$aA + xH^+ + ze^- = bB + cH_2O \tag{26}$$

where a, x, b and c are stoichiometric coefficients. If the equilibrium potential of reaction (26) is referred to the standard hydrogen electrode at the same temperature [SHE (T)], the cell reaction is

$$aA + (x-z)H^+ + (z/2)H_2 = bB + cH_2O \tag{27}$$

The equilibrium relationship for such a reaction is expressed as

$$E = E^\circ - \frac{2.303\ RT}{zF} \log \frac{[\ a_B^b\ a_{H_2O}^c]}{[\ a_A^a\ a_{H^+}^x\ ]} \tag{28}$$

where $$E^\circ = -\Delta_R G_T^\circ / zF \tag{29}$$

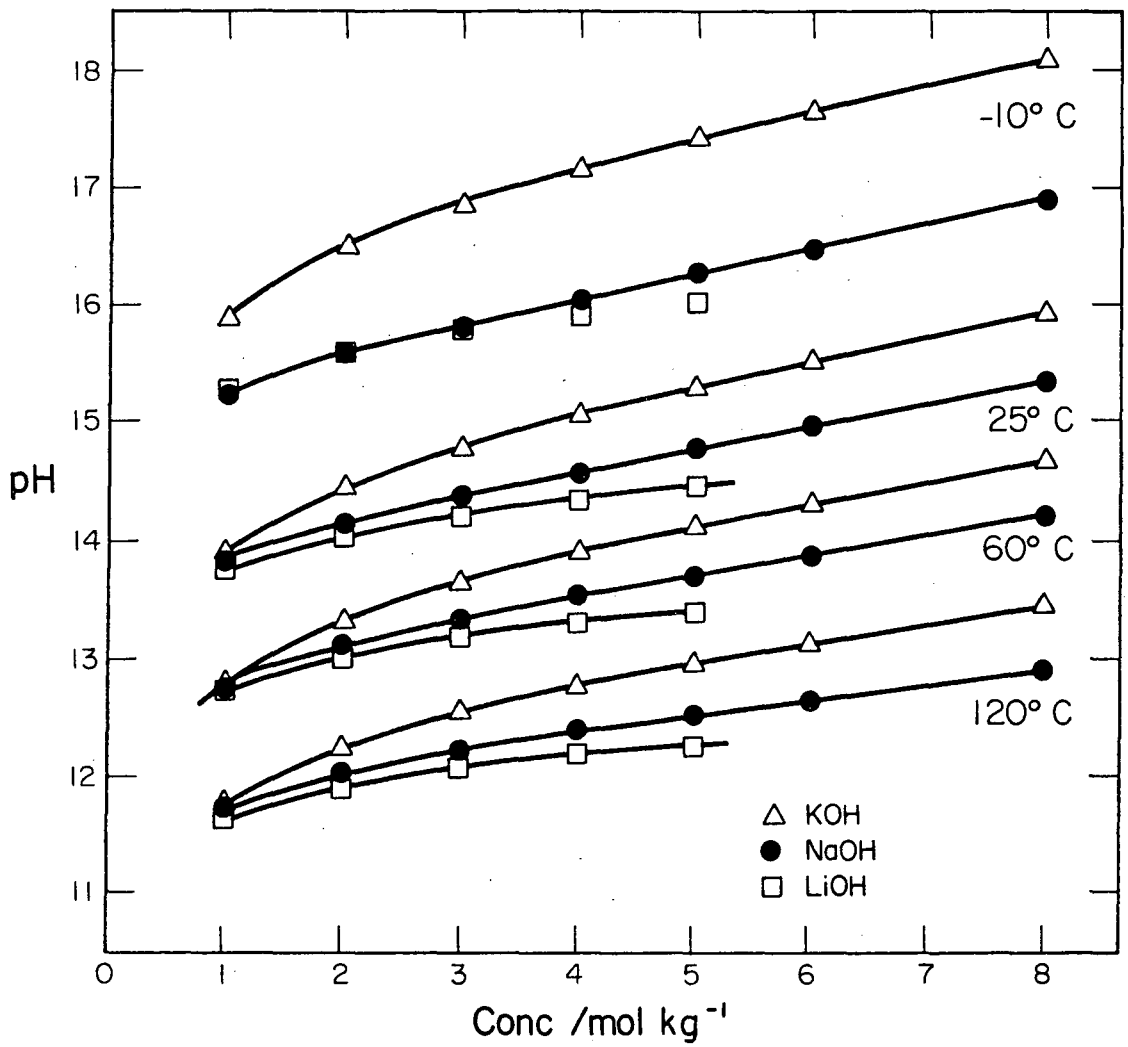

Figure 6. Variation of pH with concentration for KOH, NaOH, and LiOH solutions as a function of temperature.

$\Delta_R G_T^\circ$ denotes the change in standard free energy for reaction (27) and is given as

$$\Delta_R G_T^\circ = b\Delta_f G_B^{\circ *} + c\Delta_f G_{H_2O}^{\circ *} - a\Delta_f G_A^{\circ *} - (x-z)\Delta_f G_{H^+}^{\circ *} - (z/2)\Delta_f G_{H_2}^{\circ *} \qquad (30)$$

where $\Delta_f G_X^{\circ *}$ is the non-isothermal free energy of formation of component x at the temperature of interest. This quantity is defined in the following section.

Equation (28) can be expanded to yield

$$E = E^\circ + \frac{2.303\ RT}{zF}\,[a \log a_A - b \log a_B - c \log a_W] - \frac{2.303x\ RT}{zF}\,pH \qquad (31)$$

For reactions in which no change of oxidation state occurs, z=0 and reaction (27) reduces to

$$aA + xH^+ = bB + cH_2O \qquad (32)$$

The equilibrium condition is therefore given as

$$xpH = -(\Delta_R G_T^\circ/2.303\ RT) + a \log a_A - b \log a_B - c \log a_W \qquad (33)$$

In this work, potential-pH equations for various reactions of interest in the Li/H_2O, Al/H_2O, Zn/H_2O, Ni/H_2O, Fe/H_2O and O_2/H_2O systems were computed using the program THERM. This program was developed from a version (15) originally written to define the thermodynamics of metal/water systems under water-cooled nuclear power plant conditions. The extended program, which is available in both BASIC (Appendix C) and FORTRAN (Appendix D) code, has the facility for calculating the activity of water and the pH of each of the three hydroxide solutions. Using these data, it then computes the equilibrium potentials for each reaction at various stoichiometric concentrations of alkali hydroxide. The FORTRAN program is also capable of handling mixed oxidation products such as $Ni(FeO_2)_2$ or $NaAlO_2$. The former may be produced in an actual battery system due to transport of the soluble products from one electrode to the other. On the other hand, combination of the soluble species with an electrolyte cation will result in the second type of mixed product.

In order to provide a complete tabulation of potential-pH relationships, as given in Appendix 5, reactions involving metallic cation and oxyanion species were considered, even though only the latter are expected to be present in significant amounts in the concentrated hydroxide solutions of interest.

Evaluation of Free Energy Functions

In order to obtain the potential-pH relationship for a reaction, a method is required for calculating the change in standard free energy at the temperature of interest. In this analysis, $\Delta_R G_T^\circ$ is evaluated from the non-isothermal free energies for the species involved in the reaction as defined by Macdonald and co-workers (16,17),

$$\Delta_f G_T^{\circ *} = \Delta_f G_{298}^\circ - S_{298}^\circ(T - 298) - T\int_{298}^{T}(C_p^\circ/T)dT + \int_{298}^{T} C_p^\circ dT \qquad (34)$$

where $\Delta_f G_{298}^\circ$ is the conventional isothermal free energy of formation at 298K, S_{298}° is the absolute entropy at the reference temperature, and C_p° is the heat capacity, which is usually a function of temperature. The quantity $\Delta_f G_T^{\circ *}$ strictly refers to the free energy of formation of the compound at temperature T from its elements at 298K. It therefore differs from the isothermal free energy of formation at elevated temperatures, which is based on the convention that the free energy of an element at all temperatures is zero. Both the non-isothermal and isothermal methods of calculation lead to identical results for $\Delta_R G_T^\circ$. However, the non-isothermal approach substantially reduces the number of calculations involved.

For non-dissolved species, accurate heat capacity functions of the form

$$C_p^\circ = A + BT + CT^{-2} \qquad (35)$$

are commonly available. In contrast, there is a marked lack of directly-measured heat capacity data for dissolved ionic species. Consequently, it is usually necessary to estimate values for these species. The most widely used

method is the Criss-Cobble (18) "correspondence principle" (LIHC) approximation (10), whereby partial molal heat capacities for dissolved species are given in the form

$$\overline{C_p^\circ} = BT \tag{36}$$

Hence, the direct calculation of $\Delta_f G_T^\circ$ can be performed in general for non-dissolved and dissolved species using equation (34).

The thermodynamic data used in the present study are summarized in Appendix E and were taken whenever possible from the extensive compilation of Naumov et al (10), and from various NBS (19) and U.S. Bureau of Mines (20) tabulations. Data that were taken or calculated from other sources are summarized in Table 6, together with appropriate references and comments on the methods of evaluation.

It should be noted that there are a number of cases, mainly among the dissolved species, for which neither directly-measured nor estimated (LIHC) heat capacity data are available. For these species, C_p° has been taken as zero. In general, when heat capacity data for dissolved species are known, the conribution to $\Delta_f G_T^{\circ *}$ from the two heat capacity terms in equation (26) is less than 1% for temperatures over the range 263-393K. It is therefore assumed that where the C_p contribution is neglected, the error is sufficiently low to be acceptable in the present study.

Equilibrium Potential/Concentration Data

Equilibrium potentials for selected reactions in the systems of interest were calculated by substitution of water activity and pH data into the appropriate potential-pH equations and are presented in Appendix E. (Calculations were performed for stoichiometric alkali hydroxide concentrations over the range 1 to 8 mol kg^{-1}). For the reactions that involve dissolved reactants or products, all ionic activities have been arbitrarily set equal to 10^{-6} mol kg^{-1} in accordance with normal practice (27). This choice of activity will lead to an inherent error in the potentials of electrodes such as the $Zn(OH)_4^{2-}/Zn$ couple in battery systems which may involve quite high concentrations of soluble species. This error is specific to a particular battery system and should be taken into consideration when examining cell voltage efficiencies.

TABLE 6

THERMODYNAMIC DATA FOR SPECIES NOT LISTED IN REFERENCES (10), (19), AND (20).

Species	$\Delta_f G^\circ_{298}$ (kJ mol^{-1})	(See note a) $\bar{S}^\circ$ (JK^{-1} mol^{-1})	C_p° (JK^{-1} mol^{-1})	Comments
FeOOH	Reference (10)	Reference (10)	70.12	Calculated from "element additivity" - see note (b)
FeO_2^{2-}	-301.2 (21)	-98.16	NDA[c]	Calculated using the method of Connick and Powell. (22)
FeO_4^{2-}	-467.4	10.79	NDA	$\Delta_f G^\circ_{298}$ from Pourbaix (27)
Fe^{2+}	- 91.21	-107	NDA	
$FeOH^+$	-274.26	-33	NDA	From Tremaine et al (21).
$HFeO_2^-$	-376.35	63	NDA	
$Fe(OH)_2$ (aq)	Reference (10)	50	NDA	$\bar{S}^\circ$ estimated from plot of $\bar{S}^\circ_n$ versus n for ions $Fe(OH)_n^{2-n}$
$Ni(OH)^+$	-212.5	-50	44.3	Calculated from data of Tremaine. (23)
$Ni(OH)_2$ (aq)	-402.7	-65.1	119.6	
$HNiO_2^-$	-348.3	-214.1	119.6	
Ni_3O_4	-712.1	149.2	$129\ 035 + 0.7146 \times 10^{-1}T - 0.2393 \times 10^7\ T^{-2}$	Cowan and Staehle (24)
NiOOH	-321.7	66.9_8	66.9_0	S° and C_p° from "element additivity" - see (b). G° from $\Delta_f H^\circ$ and $\Delta_f S^\circ$ (25).
Ni_2O_3	-469.9	89.9	$98.28 + .7782 \times 10^{-1}T - 0.1435 \times 10^7\ T^{-2}$	Cowan and Staehle (24)
$Zn(OH)^+$	-341.96	64.0	40.3	Data taken from the compilation of Khodakovsky and Yelkin.
$Zn(OH)_2$(aq)	-525.09	-25.5	115.5	(26) C_p° for ions computed from pK and Y's observation
$Zn(OH)_3$	-696.64	64.9	-32.9_9	that $\Delta C_p^\circ = 0$ for ion hydrolysis.
$Zn(OH)_4^{2-}$	-861.07	17.6	-181.5	
ZnO	-320.87	43.64	Reference (10)	
- $Zn(OH)_2$	-556.05	76.99	Reference (10)	

(a) Entropy on the conventional scale where $\bar{S}^\circ_{H^+,\ 298} = 0$. Entropies in Appendix E are absolute values ($\bar{S}^\circ = \bar{S}^\circ - 20.92\ z$, where z = ion charge including sign).

(b) The entropy and particularly the heat capacity of a compound X_mY_n can be estimated from that for a compound $X_{m'}Y_{n'}$, and for either element X or Y, provided that the compounds have coordination lattices. Thus, the heat capacity of X in the reference compound is $C_p(X, ref) = [C_p(X_{m'}Y_{n'}) - n'C_p(Y)]/m'$. The heat capacity of the unknown is therefore $C_p(X_mY_n) = mC_p(X, ref) + n\ C_p(Y)$. This method has been applied successfully to estimating thermodynamic properties for the oxides of silver (17).

(c) NDA - no data available.

Previous work (7) has shown that it is more convenient to plot the calculated eqilibrium potentials against log m_{MOH} rather than pH_T as is more common. The E/pH_T plots are more complex in form than those involving log m_{MOH} owing to the variation of the activity of water and $\gamma_\pm$ with composition. Even so, the E/log m_{MOH} plots still exhibit the effect of such variations in non-linear correlations as seen, for example, in Figure 20.

The E versus log m_{MOH} diagrams for the metals of interest are given in Figures 7-21. Data are shown only for the electrode reactions desired in battery systems, and various parasitic reactions that might occur. The desired reactions considered for the five metals were as follows:

$$Li^+ + e = Li \tag{37}$$

$$Al(OH)_4^- + 3e^- = Al + 4OH^- \tag{38}$$

$$Zn(OH)_4^{2-} + 2e^- = Zn + 4OH^- \tag{39}$$

$$Fe(OH)_2 + 2e^- = Fe + 2OH^- \tag{40}$$

$$NiOOH + H_2O + e^- = Ni(OH)_2 + OH^- \tag{41}$$

In those instances where the reaction was a dissolution process, the parasitic reactions considered generally involved passivation, whereas for Ni and Fe, dissolution is a possibility. The broken line in each diagram represents the equilibrium potentials for the appropriate desired reaction. In the case of Li, Al, and Zn, the thermodynamically-favored reaction of the pure metal is the desired reaction, and the metal oxidizes directly to the pertinent species in the above reactions. However, the thermodynamically-favored reaction for Fe produces FeO_2^{2-} or, at 393K, $HFeO_2^-$. The equilibrium potentials for the Fe/FeO_2^{2-} and $Fe/HFeO_2^-$ couples were derived for an activity of 10^{-6} mol kg^{-1} for the oxyanions. In practice, the $Fe/Fe(OH)_2$ reaction would be favored if the activities of FeO_2^{2-} and $HFeO_2^-$ were sufficiently large or, more likely, the dissolution reactions were discounted for kinetic reasons.

In batteries with Ni electrodes, a $Ni/Ni(OH)_2$ couple is unsuitable as the $Ni(OH)_2$ cannot be easily reduced. Instead, the $Ni(OH)_2/NiOOH$ reaction is utilized.

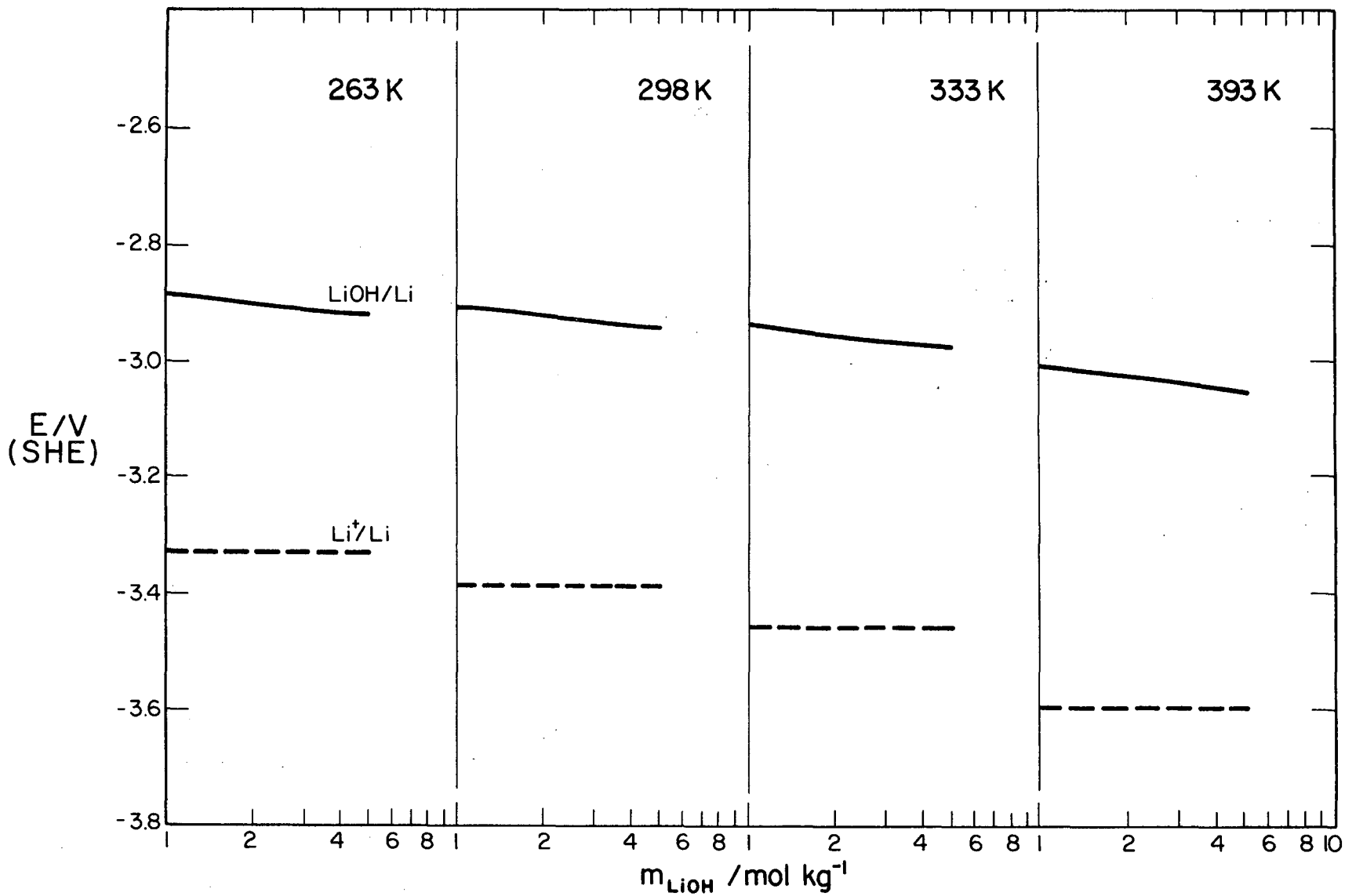

Figure 7. Potential versus log m_{LiOH} diagrams for lithium in concentrated lithium hydroxide solution as a function of temperature. $a_{Li^+} = 10^{-6}$ mol kg^{-1}

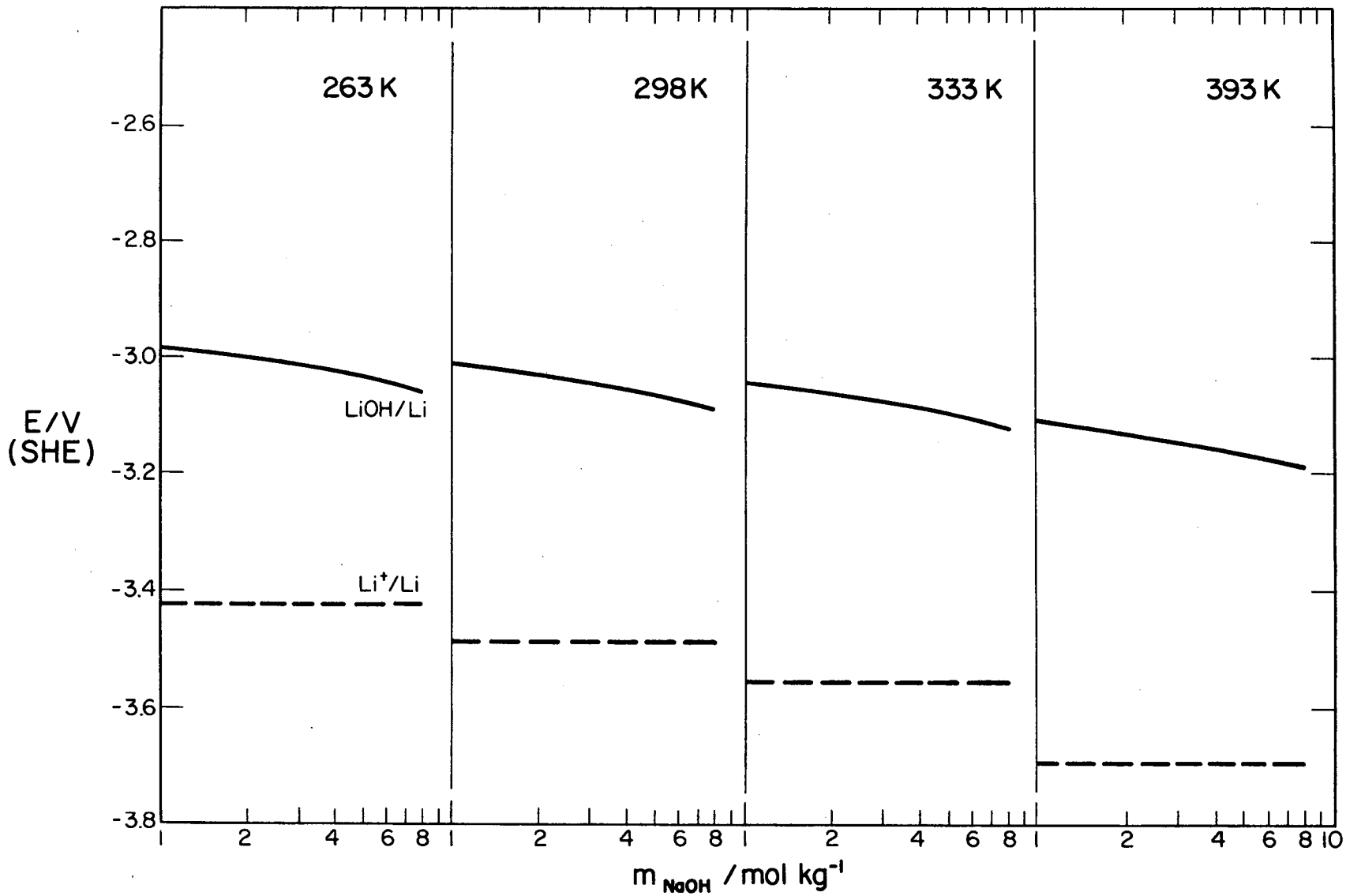

Figure 8. Potential versus log m_{NaOH} diagrams for lithium in concentrated sodium hydroxide solution as a function of temperature. $a_{Li^+} = 10^{-6}$ mol kg^{-1}

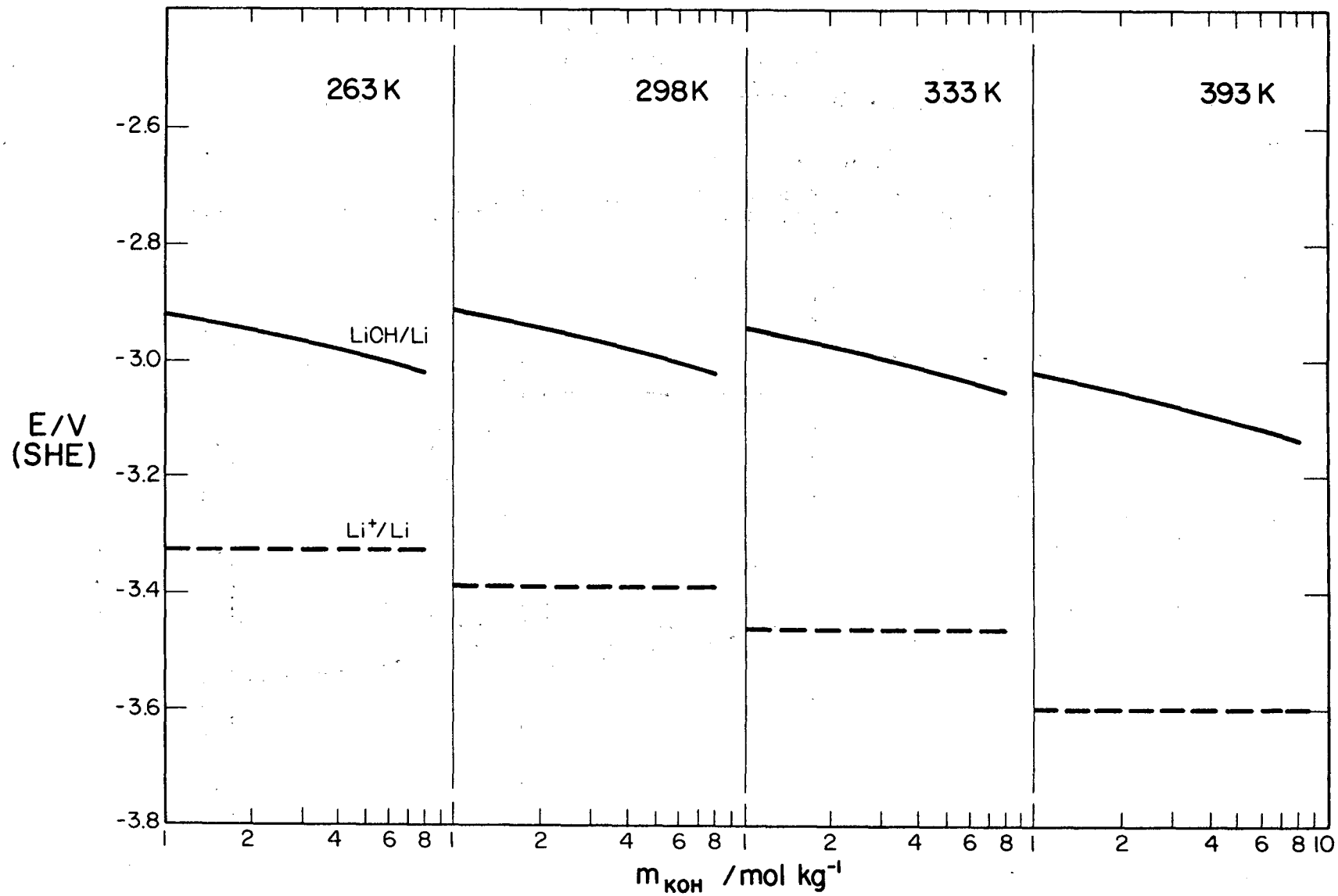

Figure 9. Potential versus log m_{KOH} diagrams for lithium in concentrated potassium hydroxide solution as a function of temperature. $a_{Li^+} = 10^{-6}$ mol kg^{-1}

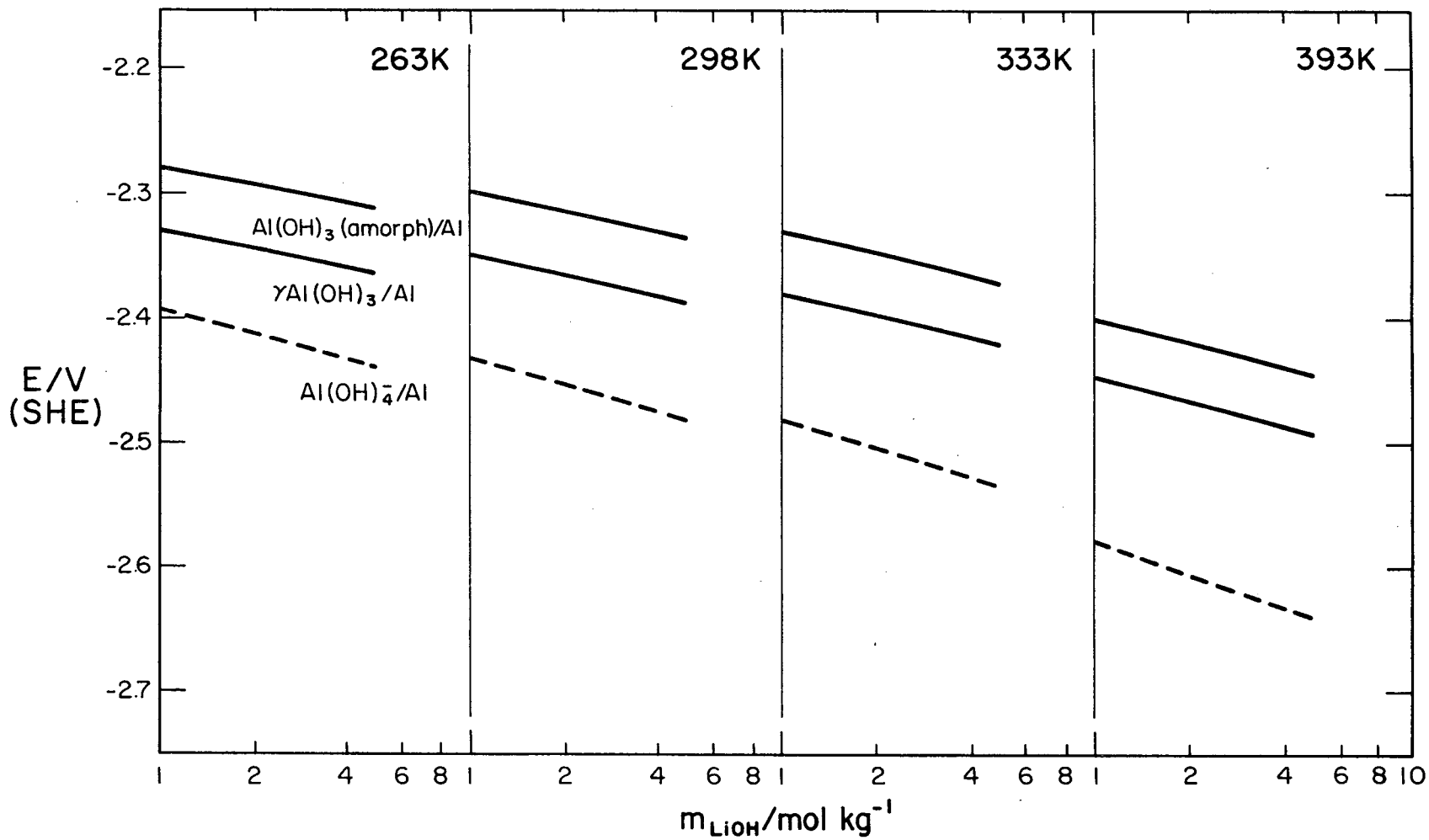

Figure 10. Potential versus log m_{LiOH} diagrams for aluminum in concentrated lithium hydroxide solution as a function of temperature. $a_{Al(OH)_4^-} = 10^{-6}$ mol kg^{-1}

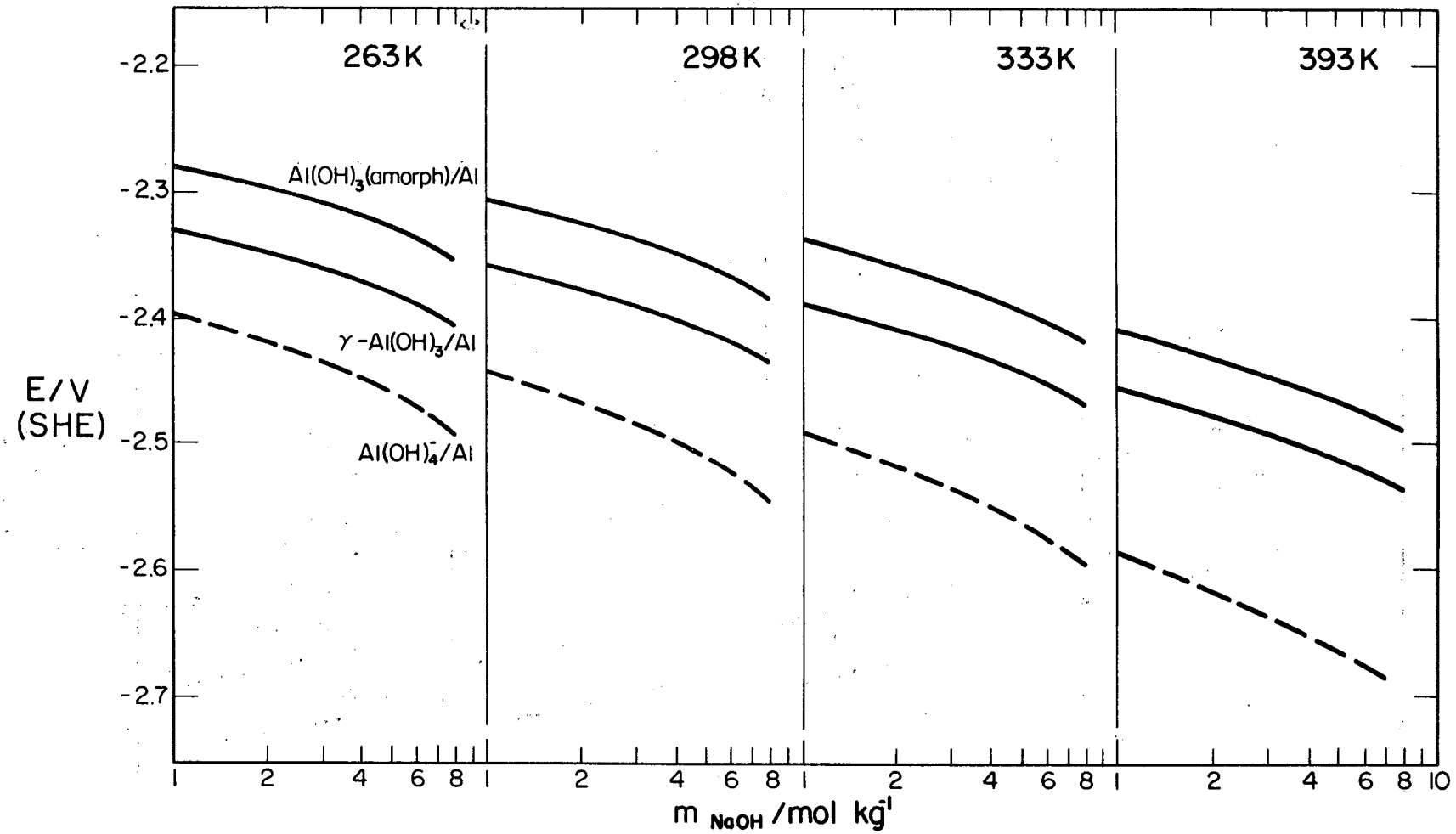

Figure 11. Potential versus log m_{NaOH} diagrams for aluminum in concentrated sodium hydroxide solution as a function of temperature. $a_{Al(OH)_4^-} = 10^{-6}$ mol kg^{-1}

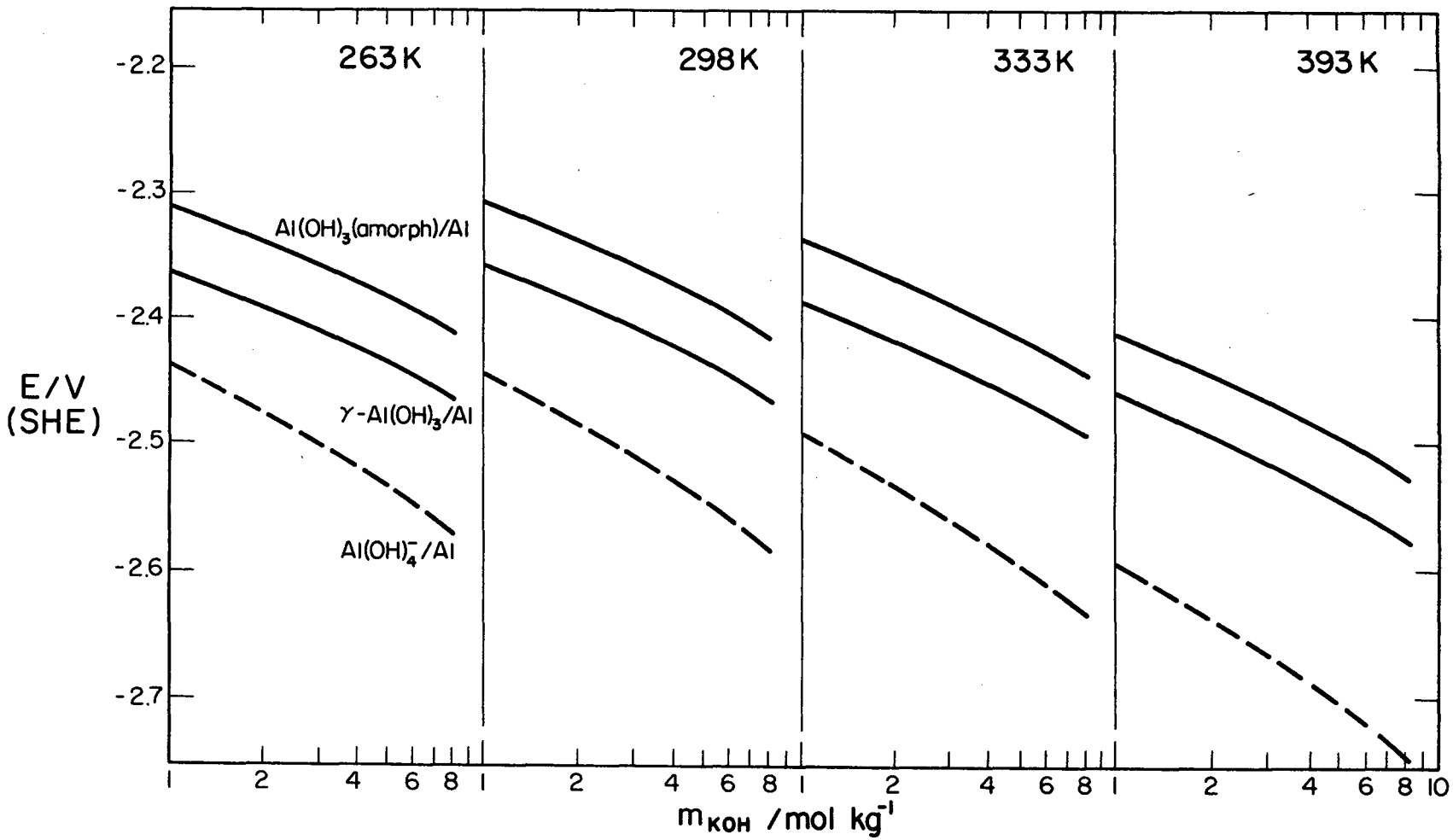

Figure 12. Potential versus log m_{KOH} diagrams for aluminum in concentrated potassium hydroxide solution as a function of temperature. $a_{Al(OH)_4^-} = 10^{-6}$ mol kg^{-1}

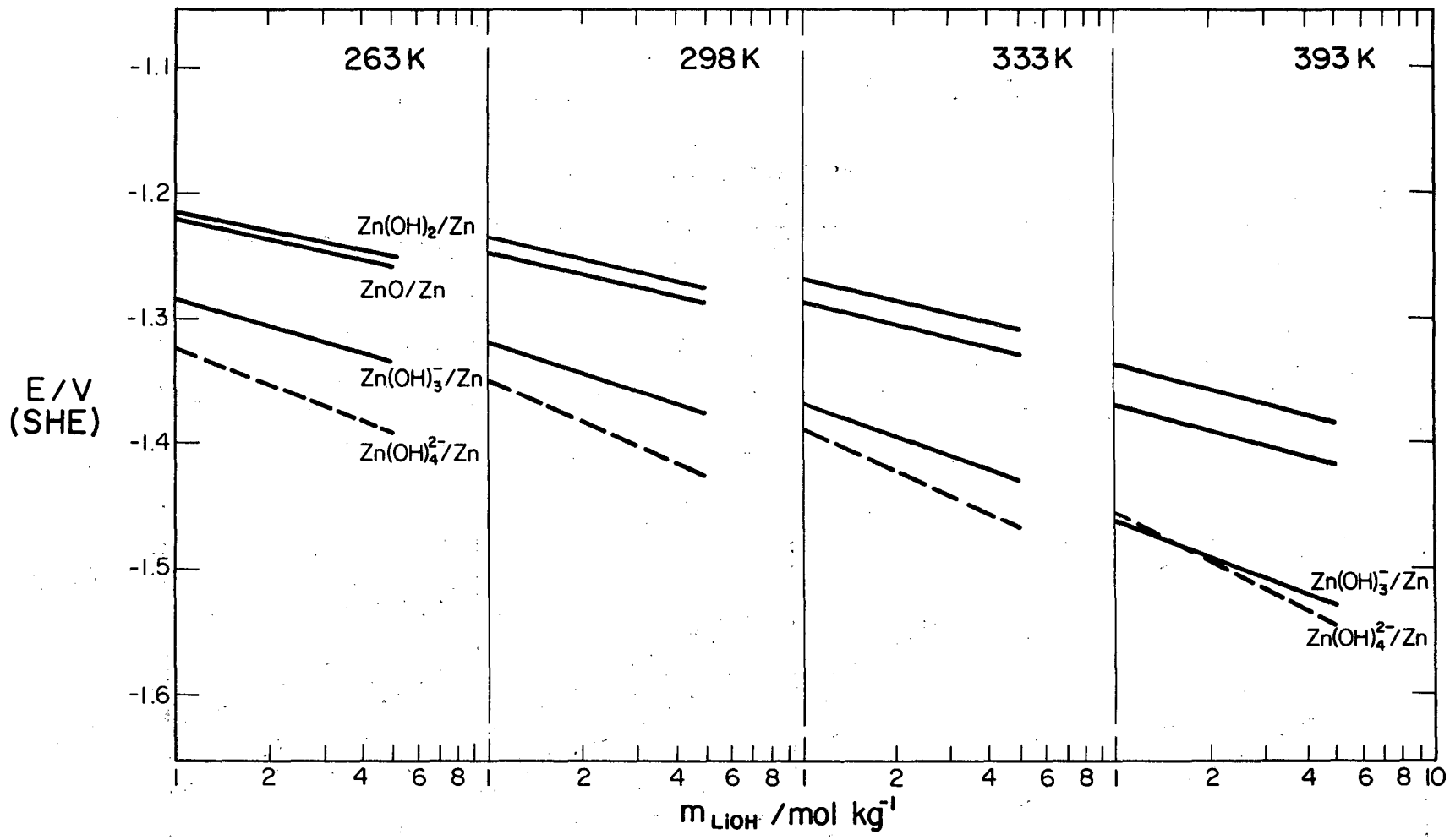

Figure 13. Potential versus log m_{LiOH} diagrams for zinc in concentrated lithium hydroxide solution as a function of temperature. $a_{Zn(OH)_3^-} = 10^{-6}$ mol kg^{-1}, $a_{Zn(OH)_4^{2-}} = 10^{-6}$ mol kg^{-1}

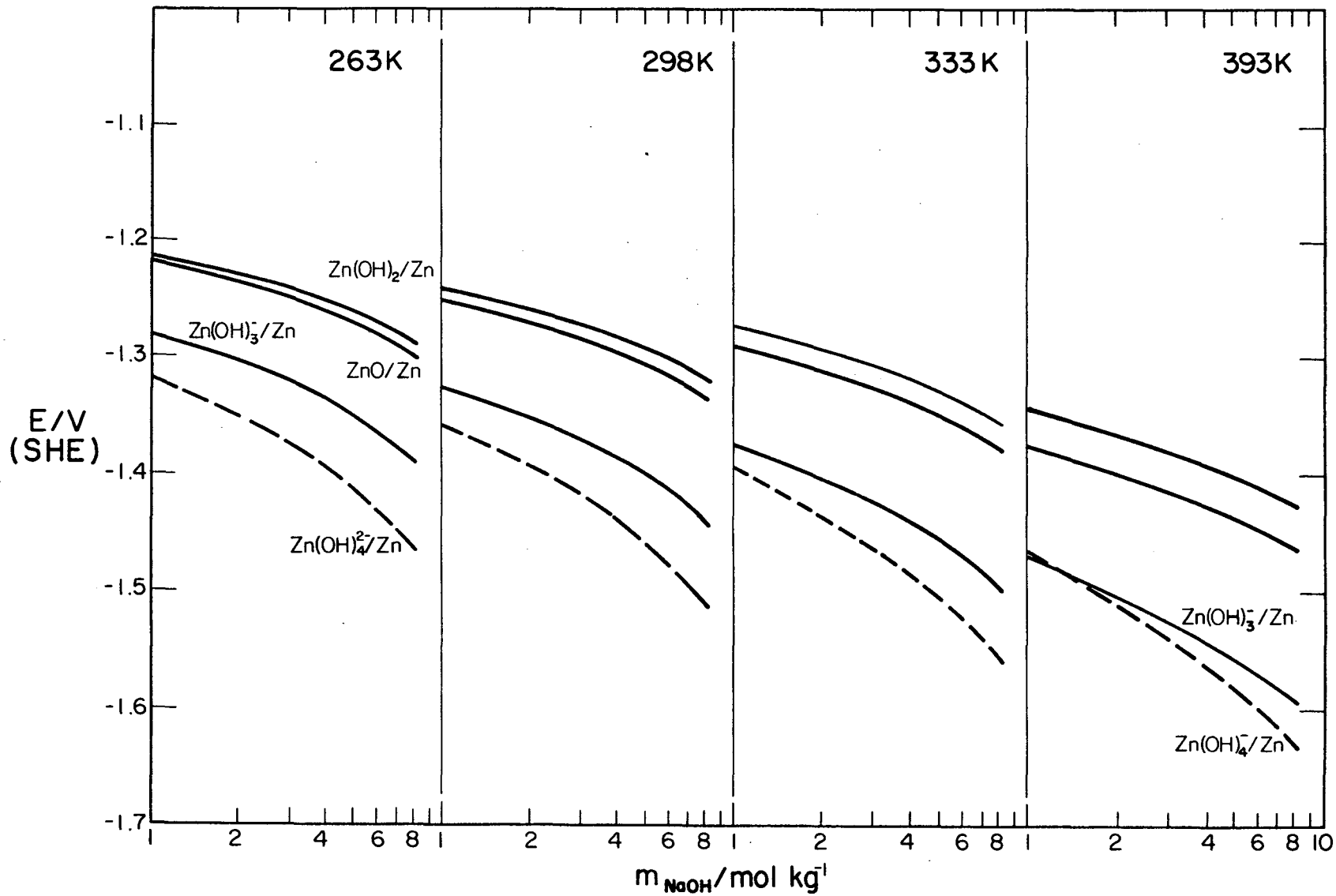

Figure 14. Potential versus log m_{NaOH} diagrams for zinc in concentrated sodium hydroxide solution as a function of temperature. $a_{Zn(OH)_3^-} = 10^{-6}$ mol kg^{-1}, $a_{ZN(OH)_4^{2-}} = 10^{-6}$ mol kg^{-1}

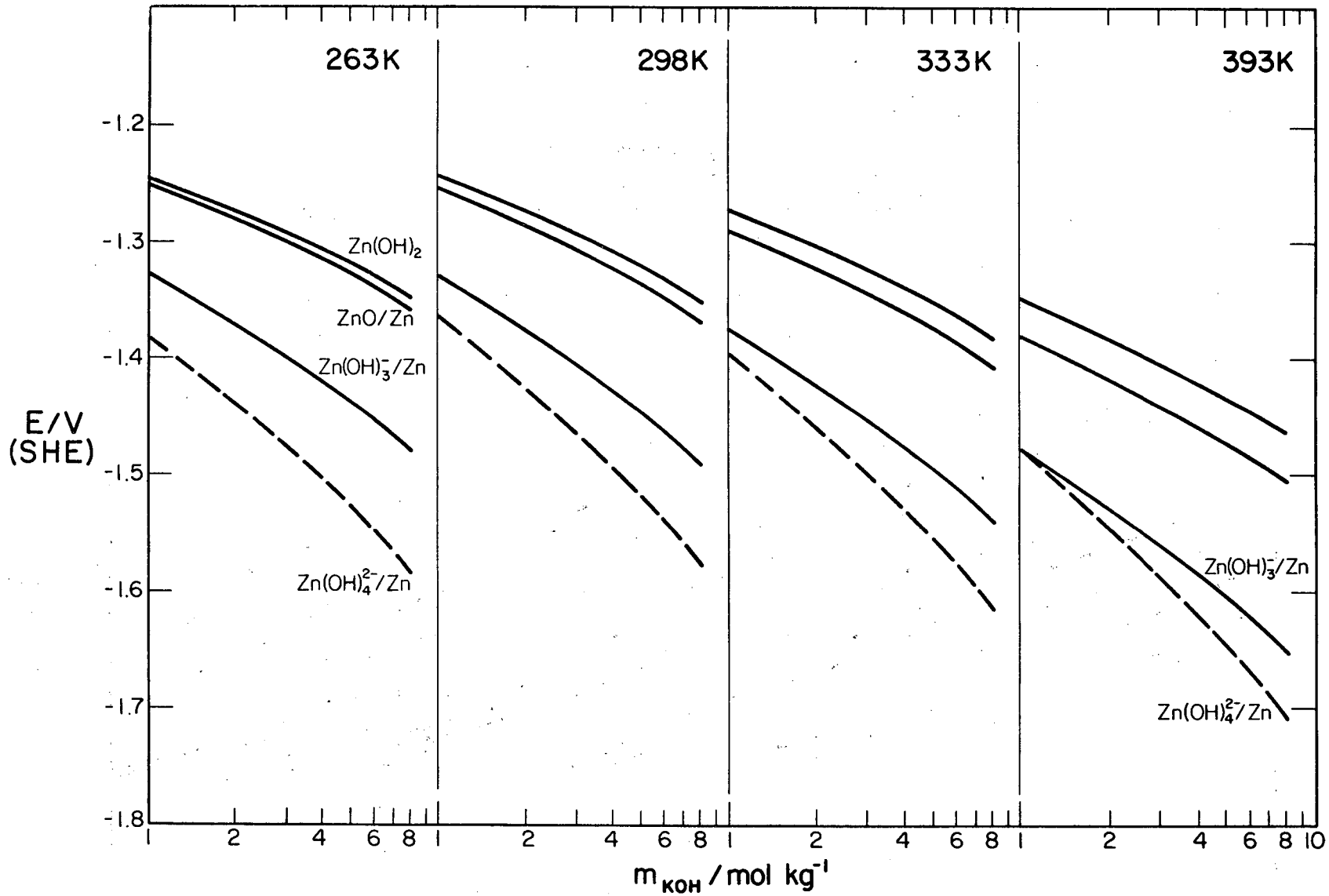

Figure 15. Potential versus log m_{KOH} diagrams for zinc in concentrated potassium hydroxide solution as a function of temperature. $a_{Zn(OH)_3^-} = 10^{-6}$ mol kg^{-1}, $a_{Zn(OH)_4^{2-}} = 10^{-6}$ mol kg^{-1}

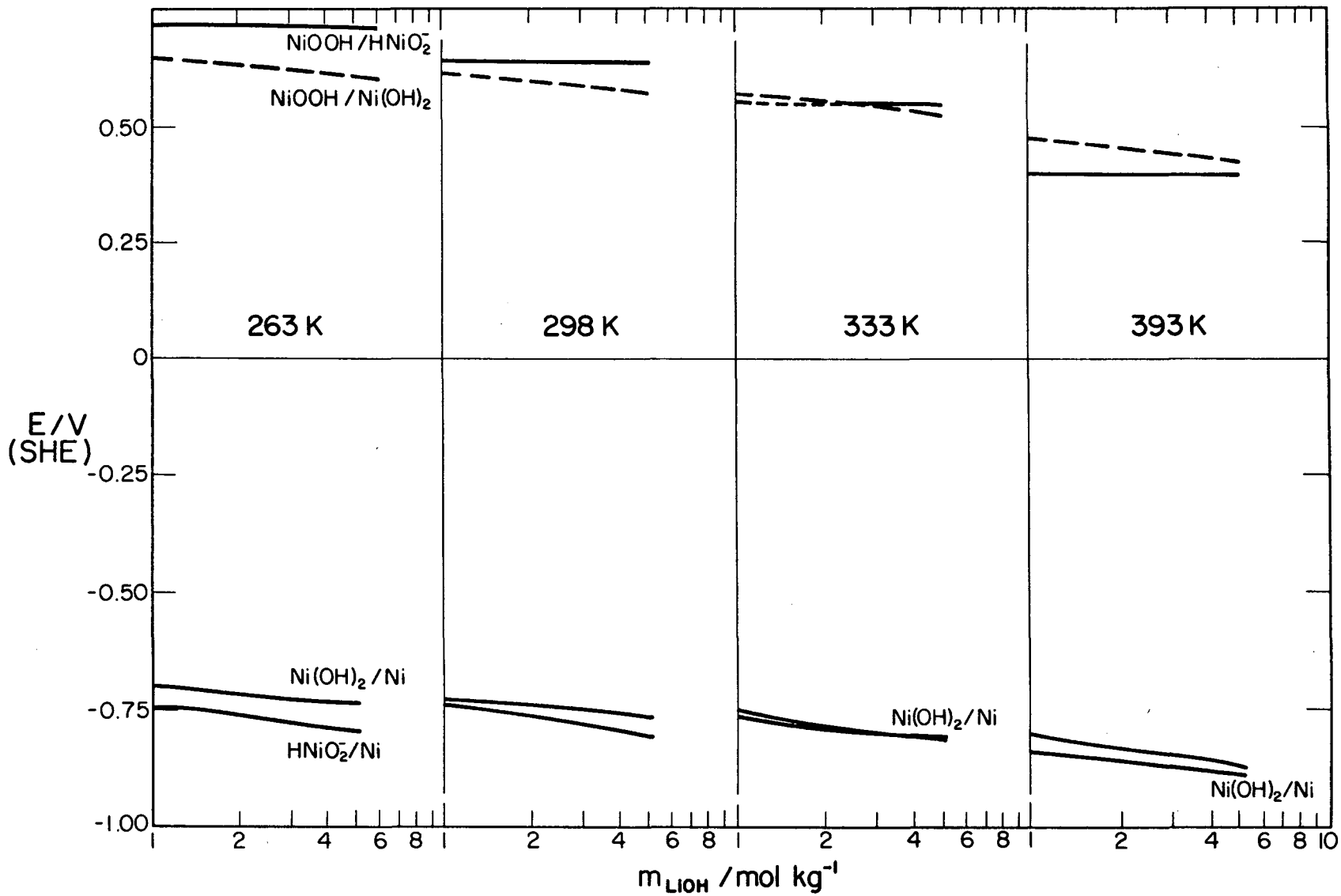

Figure 16. Potential versus log m_{LiOH} diagrams for nickel in concentrated lithium hydroxide solution.
$a_{HNiO_2^-} = 10^{-6}$ mol kg^{-1}

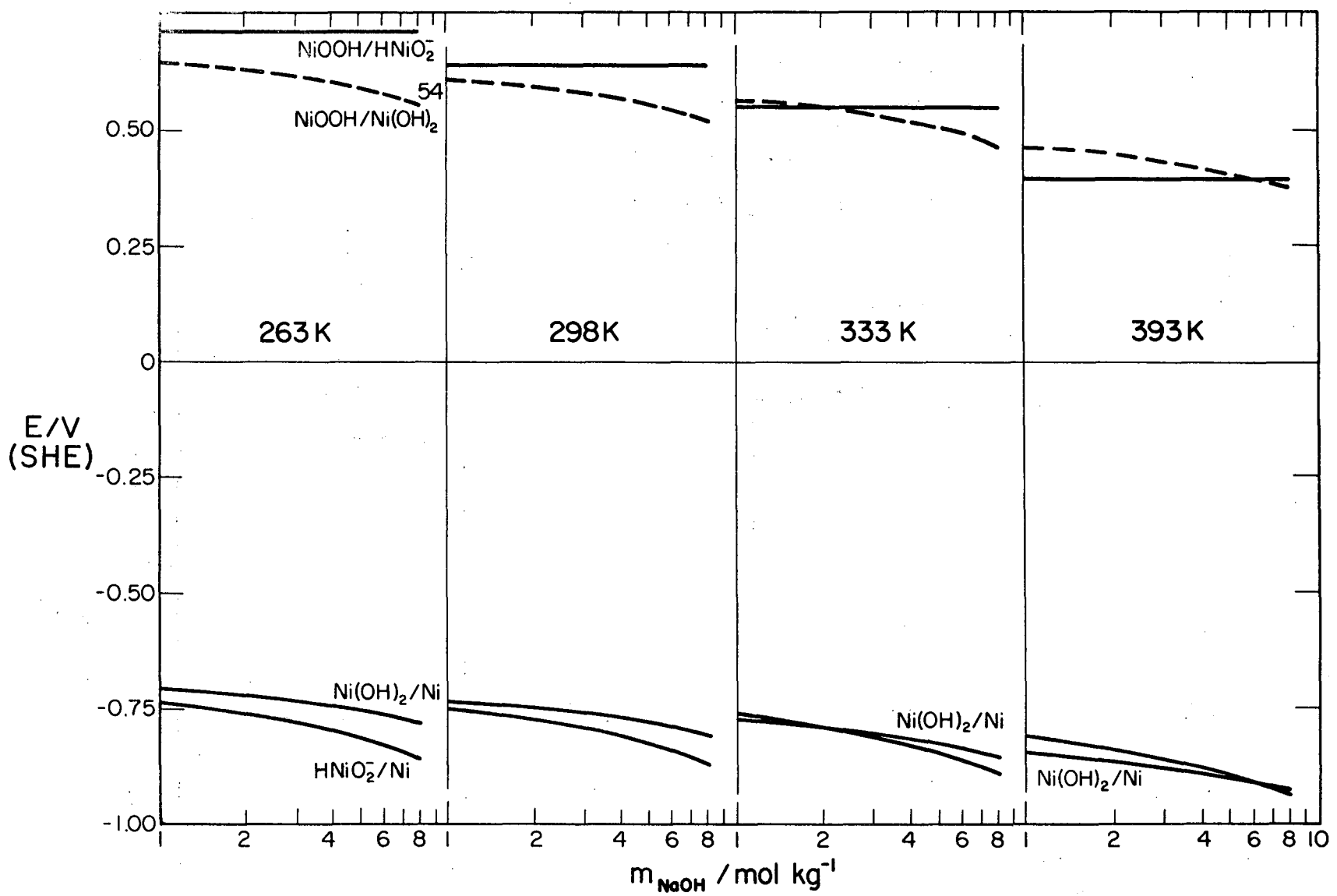

Figure 17. Potential versus log m_{NaOH} diagrams for nickel in concentrated sodium hydroxide solution as a function of temperature. $a_{HNiO_2^-} = 10^{-6}$ mol kg^{-1}

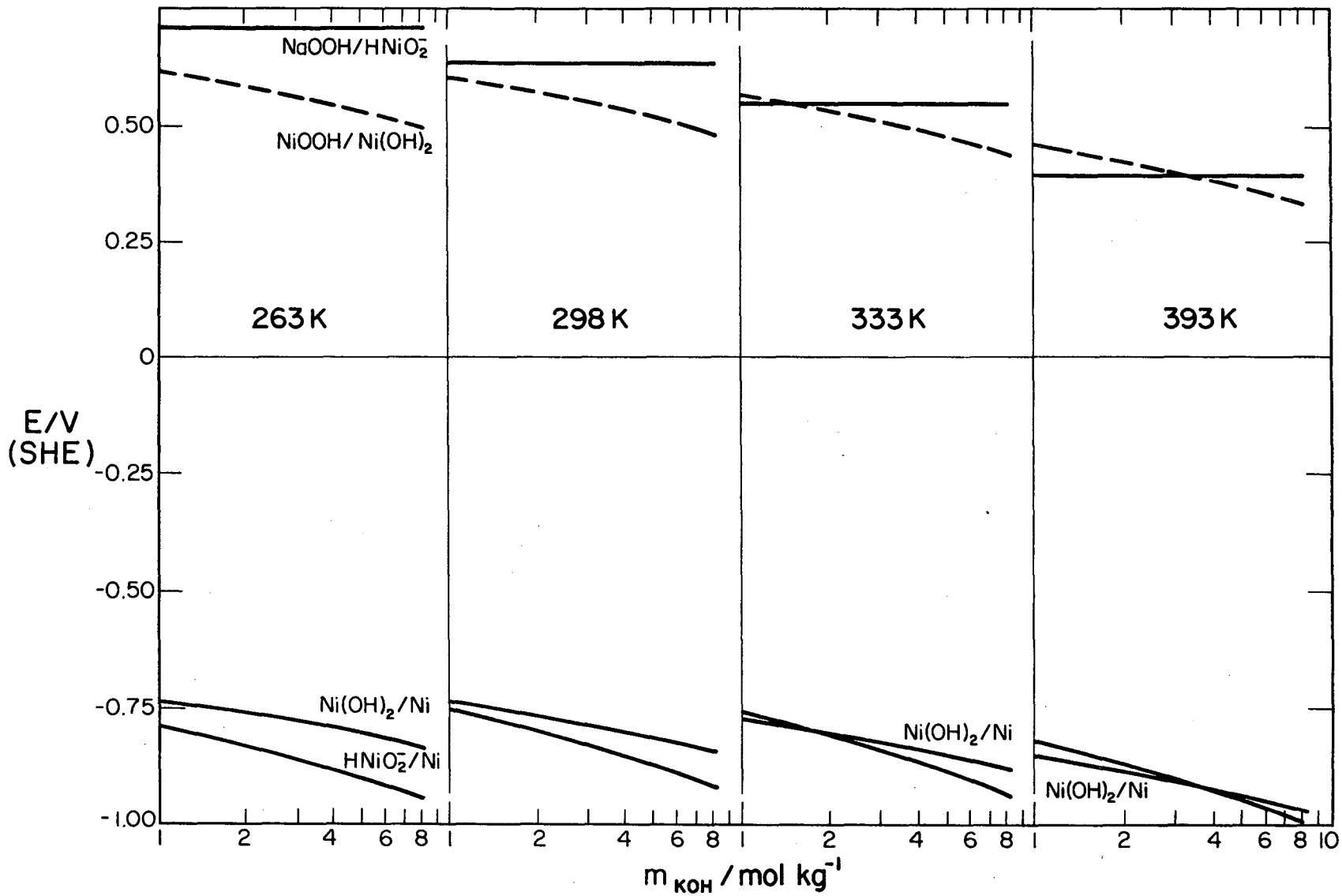

Figure 18. Potential versus log m_{KOH} diagrams for nickel in concentrated potassium hydroxide solution as a function of temperature. $a_{HNiO_2^-} = 10^{-6}$ mol kg^{-1}

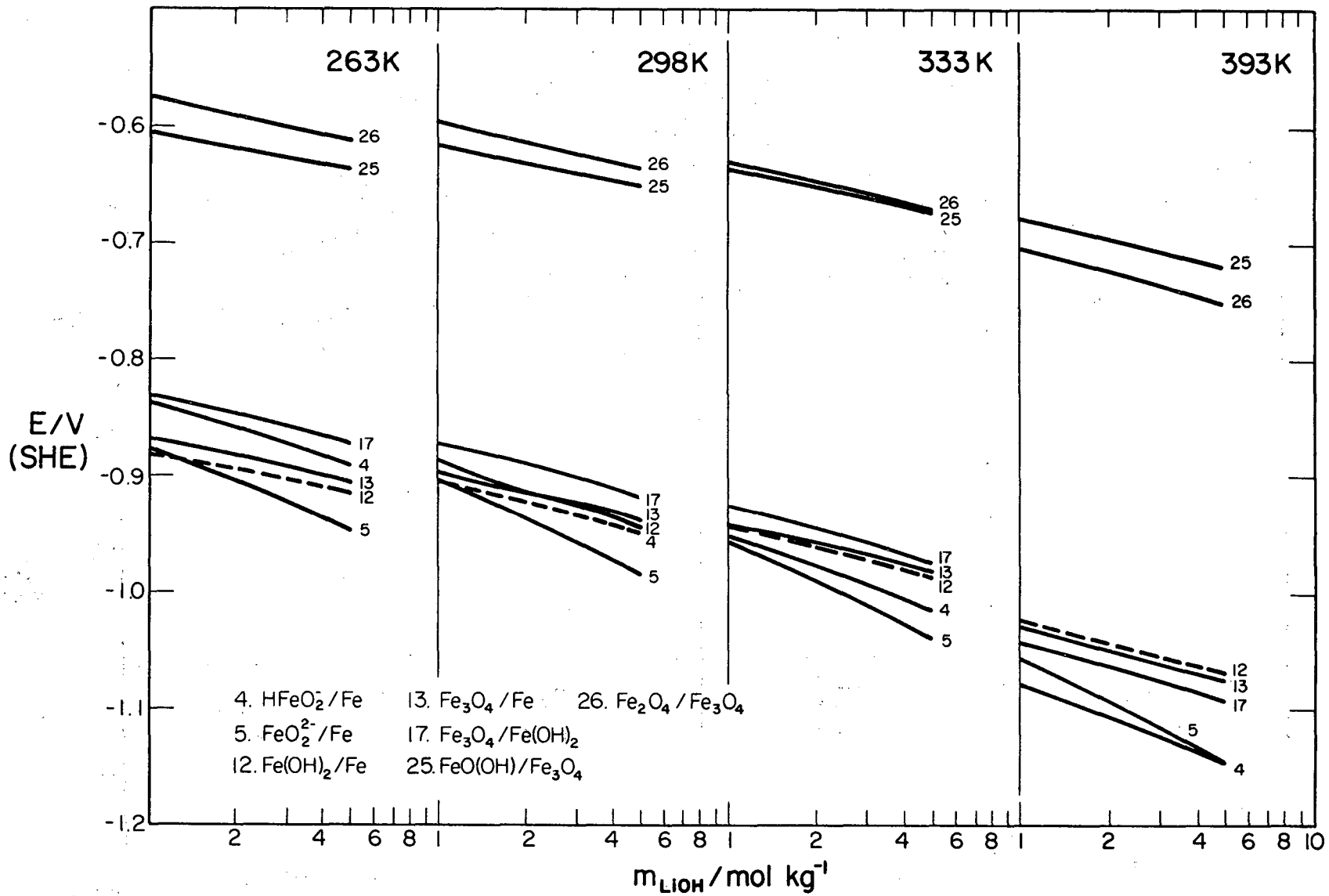

Figure 19. Potential versus log m_{LiOH} diagrams for iron in concentrated lithium hydroxide solution as a function of temperature.

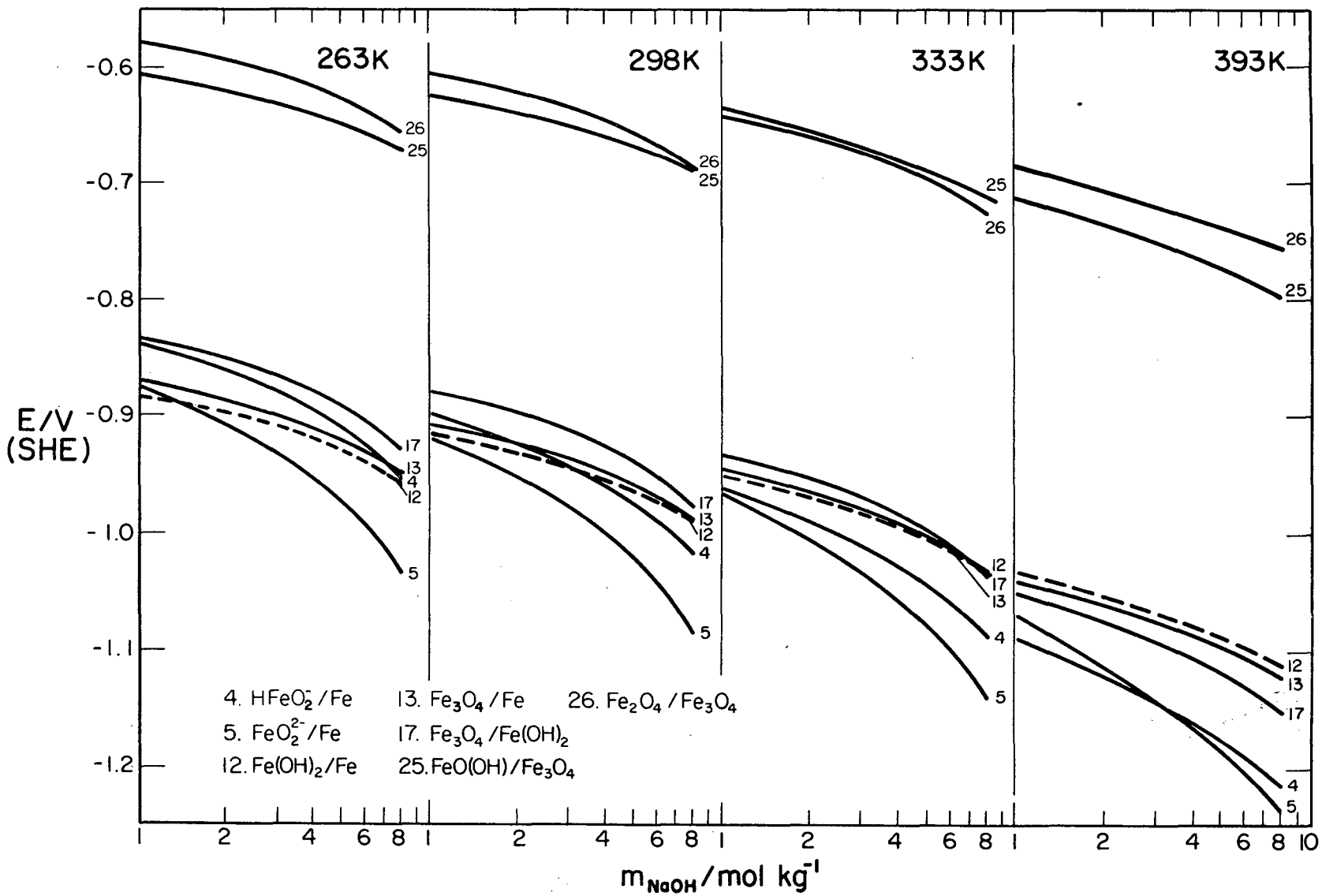

Figure 20. Potential versus log m_{NaOH} diagrams for iron in concentrated sodium hydroxide solution as a function of temperature.

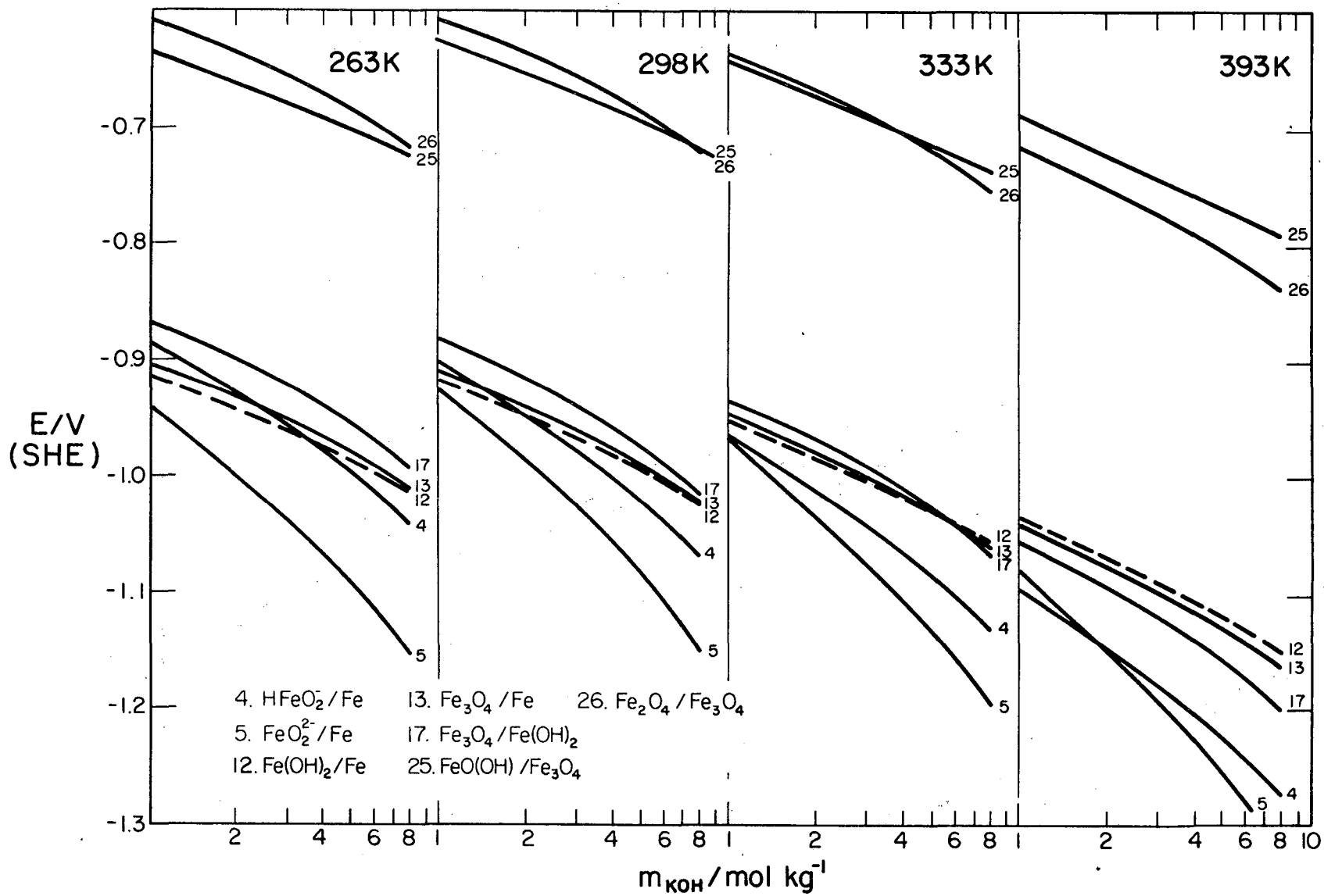

Figure 21. Potential versus log $_{mKOH}$ diagrams for iron in concentrated potassium hydroxide solution as a function of temperature.

The E/log m_{MOH} diagrams for Zn and Fe exhibit changes in the relative positions of the metal/anion equilibria curves with increasing temperature. The curves associated with $HFeO_2^-$ and $Zn(OH)_3^-$ move closer to those for FeO_2^{2-} and $Zn(OH)_4^{2-}$, respectively, with the two pairs of curves intersecting at 393K. Therefore, each anion in both cases at this temperature predominant over a part of the concentration range shown. In the case of Zn, the $Zn(OH)_4^{2-}$ ion still prevails over most of that range but does so to a decreasing extent over the series KOH>NaOH>LiOH. The effect of temperature in the diagram for Fe is more marked such that at 393K, $HFeO_2^-$ replaces FeO_2^{2-} as the predominant anion for most of the concentration range. This change of anion reflects both a decrease in pK_a for $HFeO_2^-$ and a lowering of the pH of the medium with increasing temperature.

THERMODYNAMICS OF ALKALINE BATTERIES

Cell Potentials

The various batteries of practical interest can be separated into two broad groups:

i) metal/air systems where the metal can be Li, Al, Zn, and Fe,

ii) M/Ni systems where M=Fe, Zn, or H_2.

The reactions considered to be taking place at the metal electrodes are given by equations 37-41 while the air and H_2 electrodes involve reactions 34 and 35 respectively.

$$O_2 + 2H_2O + 4e^- = 4OH^- \tag{42}$$

$$2H_2O + 2e^- = H_2 + 2OH^- \tag{43}$$

Using the data given in Appendix E, cell potentials for the above systems were obtained for each concentration and temperature and these are given in Tables 7-14. The cell potentials for the Al/air, Zn/air and Zn/Ni systems were found to increase with concentration, where the magnitude of the increase over the range 1 to 5mol kg^{-1} follows the order KOH> NaOH> LiOH. In contrast, at each concentration, the cell potentials decrease as the temperature increases.

TABLE 7

EQUILIBRIUM POTENTIALS FOR Li/AIR CELL
IN CONCENTRATED ALKALI HYDROXIDE SOLUTIONS
(P_{O_2} = 0.2 atm, $a_{Li^+} = 10^{-6}$ mol kg^{-1})

m/mol kg^{-1}	Temperature/K							
	263	273	298	313	333	353	373	393
LiOH								
1	3.777	3.786	3.794	3.799	3.805	3.813	3.820	3.827
2	3.762	3.770	3.778	3.782	3.788	3.795	3.801	3.807
3	3.754	3.761	3.767	3.772	3.777	3.784	3.789	3.796
4	3.747	3.754	3.760	3.764	3.769	3.776	3.780	3.787
5	3.741	3.748	3.754	3.758	3.763	3.769	3.773	3.781
NaOH								
1	3.778	3.782	3.788	3.794	3.801	3.807	3.814	3.821
2	3.763	3.766	3.771	3.776	3.781	3.787	3.792	3.798
3	3.751	3.754	3.758	3.762	3.767	3.772	3.777	3.783
4	3.740	3.742	3.747	3.750	3.755	3.760	3.765	3.771
5	3.729	3.732	3.736	3.739	3.744	3.749	3.754	3.761
6	3.719	3.721	3.725	3.729	3.733	3.739	3.745	3.751
8	3.699	3.701	3.705	3.709	3.713	3.720	3.726	3.734
KOH								
1	3.745	3.786	3.786	3.791	3.800	3.805	3.811	3.816
2	3.716	3.757	3.754	3.760	3.768	3.772	3.777	3.781
3	3.698	3.739	3.734	3.741	3.747	3.751	3.755	3.759
4	3.683	3.725	3.719	3.726	3.731	3.735	3.738	3.742
5	3.671	3.713	3.706	3.713	3.718	3.721	3.725	3.728
6	3.660	3.703	3.694	3.702	3.706	3.709	3.712	3.715
8	3.639	3.683	3.672	3.681	3.685	3.687	3.690	3.693

TABLE 8

EQUILIBRIUM POTENTIALS FOR Al/AIR CELL IN CONCENTRATED ALKALI HYDROXIDE SOLUTIONS

(P_{O_2} = 0.2 atm, $a_{Al(OH)_4^-}$ = 10^{-6} mol kg^{-1})

m/mol kg^{-1}	Temperature/K							
	263	273	298	313	333	353	373	393
LiOH								
1	2.848	2.844	2.840	2.836	2.831	2.825	2.818	2.811
2	2.852	2.849	2.844	2.841	2.836	2.830	2.824	2.817
3	2.854	2.852	2.847	2.844	2.839	2.833	2.827	2.821
4	2.856	2.853	2.849	2.846	2.841	2.835	2.830	2.823
5	2.857	2.855	2.851	2.847	2.843	2.837	2.831	2.824
NaOH								
1	2.847	2.845	2.841	2.838	2.832	2.827	2.820	2.813
2	2.852	2.850	2.846	2.843	2.838	2.833	2.827	2.820
3	2.855	2.854	2.850	2.847	2.842	2.837	2.831	2.824
4	2.858	2.857	2.853	2.850	2.845	2.840	2.834	2.827
5	2.860	2.859	2.855	2.852	2.848	2.842	2.837	2.830
6	2.863	2.861	2.858	2.855	2.850	2.845	2.839	2.832
8	2.866	2.865	2.861	2.858	2.854	2.848	2.842	2.835
KOH								
1	2.858	2.844	2.842	2.838	2.832	2.827	2.821	2.815
2	2.866	2.853	2.852	2.848	2.842	2.837	2.831	2.825
3	2.871	2.858	2.857	2.853	2.848	2.843	2.838	2.832
4	2.875	2.861	2.861	2.857	2.852	2.847	2.842	2.836
5	2.878	2.864	2.864	2.860	2.855	2.850	2.845	2.838
6	2.880	2.866	2.867	2.862	2.858	2.853	2.848	2.842
8	2.884	2.870	2.871	2.866	2.862	2.857	2.852	2.846

TABLE 9

EQUILIBRIUM POTENTIALS FOR Zn/AIR CELL
IN CONCENTRATED SLKALI HYDROXIDE SOLUTIONS
(P_{O_2} = 0.2 atm, $a_{Zn(OH)_4^{2-}} = 10^{-6}$ mol kg^{-1})

m/mol kg^{-1}	Temperature/K							
	263	273	298	313	333	353	373	393
LiOH								
1	1.773	1.764	1.754	1.746	1.734	1.719	1.703	1.685
2	1.787	1.779	1.769	1.762	1.750	1.736	1.721	1.704
3	1.795	1.788	1.778	1.771	1.760	1.746	1.732	1.715
4	1.801	1.794	1.785	1.778	1.766	1.753	1.739	1.722
5	1.805	1.799	1.790	1.783	1.772	1.759	1.745	1.728
NaOH								
1	1.772	1.768	1.759	1.750	1.738	1.724	1.709	1.692
2	1.786	1.783	1.775	1.767	1.756	1.744	1.729	1.713
3	1.797	1.794	1.787	1.780	1.769	1.757	1.743	1.727
4	1.807	1.804	1.797	1.790	1.780	1.768	1.753	1.737
5	1.816	1.813	1.807	1.800	1.790	1.777	1.763	1.746
6	1.824	1.822	1.815	1.808	1.798	1.785	1.771	1.754
8	1.840	1.837	1.831	1.824	1.814	1.800	1.785	1.767
KOH								
1	1.804	1.764	1.761	1.753	1.738	1.726	1.711	1.696
2	1.831	1.791	1.791	1.782	1.769	1.758	1.744	1.730
3	1.848	1.808	1.810	1.800	1.788	1.777	1.764	1.750
4	1.861	1.820	1.823	1.813	1.802	1.791	1.778	1.765
5	1.872	1.830	1.834	1.824	1.813	1.803	1.790	1.777
6	1.881	1.839	1.844	1.834	1.823	1.813	1.800	1.787
8	1.897	1.854	1.861	1.850	1.840	1.830	1.818	1.804

TABLE 10

EQUILIBRIUM POTENTIALS FOR Fe/AIR CELL
IN CONCENTRATED ALKALI HYDROXIDE SOLUTIONS
(P_{O_2} = 0.2 ATM)

m/mol kg^{-1}	Temperature/K							
	263	273	298	313	333	353	373	393
LiOH								
1	1.334	1.329	1.314	1.305	1.293	1.281	1.268	1.255
2	1.334	1.328	1.314	1.305	1.293	1.281	1.268	1.255
3	1.334	1.328	1.313	1.304	1.292	1.280	1.267	1.254
4	1.333	1.328	1.313	1.304	1.292	1.279	1.267	1.254
5	1.333	1.327	1.313	1.304	1.291	1.279	1.266	1.253
NaOH								
1	1.334	1.329	1.314	1.305	1.293	1.281	1.268	1.255
2	1.334	1.328	1.314	1.305	1.293	1.280	1.268	1.255
3	1.334	1.328	1.313	1.304	1.292	1.280	1.267	1.254
4	1.333	1.327	1.313	1.303	1.291	1.279	1.266	1.253
5	1.332	1.326	1.312	1.303	1.290	1.278	1.265	1.253
6	1.331	1.325	1.311	1.302	1.290	1.277	1.265	1.252
8	1.329	1.323	1.309	1.300	1.287	1.275	1.262	1.250
KOH								
1	1.334	1.329	1.314	1.305	1.293	1.281	1.268	1.255
2	1.333	1.328	1.313	1.305	1.292	1.280	1.267	1.254
3	1.332	1.327	1.313	1.304	1.291	1.279	1.266	1.253
4	1.332	1.327	1.312	1.303	1.290	1.278	1.265	1.252
5	1.331	1.326	1.311	1.302	1.290	1.277	1.264	1.251
6	1.330	1.325	1.310	1.301	1.288	1.276	1.263	1.250
8	1.327	1.322	1.307	1.298	1.286	1.273	1.261	1.248

TABLE 11

EQUILIBRIUM POTENTIALS FOR Zn/Ni CELL
IN CONCENTRATED ALKALI SOLUTIONS

($a_{Zn(OH)_4^{2-}} = 10^{-6}$ mol kg^{-1})

m/mol kg^{-1}	Temperature/K							
	263	273	298	313	333	353	373	393
LiOH								
1	1.962	1.958	1.958	1.956	1.952	1.945	1.936	1.926
2	1.975	1.972	1.973	1.971	1.968	1.961	1.953	1.944
3	1.983	1.980	1.981	1.980	1.977	1.971	1.964	1.954
4	1.988	1.986	1.988	1.987	1.983	1.977	1.971	1.961
5	1.992	1.990	1.992	1.992	1.988	1.983	1.977	1.966
NaOH								
1	1.961	1.961	1.963	1.960	1.956	1.950	1.942	1.932
2	1.975	1.976	1.979	1.977	1.974	1.969	1.962	1.952
3	1.985	1.987	1.990	1.989	1.986	1.981	1.975	1.965
4	1.994	1.996	2.000	1.999	1.996	1.991	1.985	1.975
5	2.002	2.004	2.008	2.007	2.005	2.000	1.993	1.983
6	2.010	2.012	2.016	2.015	2.013	2.007	2.000	1.990
8	2.023	2.025	2.029	2.028	2.026	2.020	2.012	2.002
KOH								
1	1.992	1.957	1.965	1.963	1.956	1.952	1.944	1.936
2	2.019	1.984	1.994	1.991	1.986	1.982	1.976	1.969
3	2.035	1.999	2.012	2.009	2.004	2.001	1.995	1.988
4	2.047	2.011	2.025	2.021	2.017	2.014	2.009	2.002
5	2.056	2.020	2.035	2.031	2.028	2.025	2.019	2.013
6	2.065	2.028	2.043	2.039	2.036	2.034	2.028	2.022
8	2.078	2.041	2.058	2.053	2.051	2.048	2.043	2.037

TABLE 12

EQUILIBRIUM POTENTIALS FOR Fe/Ni CELL
IN CONCENTRATED ALKALI HYDROXIDE SOLUTIONS

m/mol kg^{-1}	Temperature/K							
	263	273	298	313	333	353	373	393
LiOH								
1	1.523	1.522	1.518	1.515	1.511	1.507	1.501	1.495
2	1.522	1.521	1.517	1.515	1.511	1.506	1.500	1.494
3	1.522	1.520	1.517	1.514	1.510	1.505	1.499	1.493
4	1.521	1.520	1.516	1.513	1.509	1.504	1.498	1.492
5	1.520	1.519	1.515	1.512	1.508	1.503	1.497	1.491
NaOH								
1	1.523	1.522	1.518	1.515	1.511	1.506	1.501	1.495
2	1.522	1.521	1.517	1.515	1.510	1.505	1.500	1.494
3	1.521	1.520	1.516	1.513	1.509	1.504	1.499	1.493
4	1.520	1.519	1.515	1.512	1.508	1.503	1.497	1.491
5	1.518	1.517	1.513	1.510	1.506	1.501	1.496	1.490
6	1.517	1.515	1.511	1.508	1.504	1.500	1.494	1.488
8	1.512	1.511	1.507	1.504	1.500	1.495	1.490	1.484
KOH								
1	1.522	1.522	1.518	1.515	1.511	1.506	1.501	1.495
2	1.521	1.521	1.516	1.514	1.510	1.505	1.499	1.493
3	1.519	1.519	1.515	1.512	1.508	1.503	1.497	1.491
4	1.517	1.517	1.513	1.510	1.506	1.501	1.496	1.489
5	1.516	1.516	1.511	1.508	1.504	1.499	1.493	1.487
6	1.514	1.514	1.509	1.506	1.502	1.497	1.491	1.485
8	1.509	1.509	1.504	1.502	1.497	1.492	1.486	1.480

TABLE 13

EQUILIBRIUM POTENTIALS FOR H_2/Ni CELL
IN CONCENTRATED ALKALI HYDROXIDE SOLUTIONS
(Discharged Condition, P_{H_2} assumed to be 1 atm)

m/mol kg^{-1}	Temperature/K							
	263	273	298	313	333	353	373	393
LiOH								
1	1.439	1.435	1.423	1.416	1.407	1.397	1.388	1.378
2	1.439	1.435	1.423	1.416	1.407	1.397	1.388	1.378
3	1.439	1.435	1.423	1.416	1.407	1.398	1.388	1.378
4	1.439	1.435	1.423	1.416	1.407	1.398	1.388	1.378
5	1.439	1.435	1.423	1.416	1.407	1.398	1.388	1.378
NaOH								
1	1.439	1.435	1.423	1.416	1.407	1.397	1.388	1.378
2	1.439	1.435	1.423	1.416	1.407	1.397	1.388	1.378
3	1.439	1.435	1.423	1.416	1.407	1.397	1.388	1.378
4	1.439	1.435	1.423	1.416	1.407	1.397	1.388	1.378
5	1.439	1.435	1.423	1.416	1.407	1.397	1.388	1.378
6	1.439	1.435	1.423	1.416	1.407	1.397	1.388	1.378
8	1.439	1.435	1.423	1.416	1.407	1.397	1.388	1.378
KOH								
1	1.439	1.435	1.423	1.416	1.407	1.397	1.388	1.378
2	1.439	1.435	1.423	1.416	1.407	1.397	1.388	1.378
3	1.439	1.435	1.423	1.416	1.407	1.397	1.388	1.378
4	1.439	1.435	1.423	1.416	1.407	1.397	1.388	1.378
5	1.439	1.435	1.423	1.416	1.407	1.397	1.388	1.378
6	1.439	1.435	1.423	1.416	1.407	1.397	1.388	1.378
8	1.439	1.435	1.423	1.416	1.407	1.397	1.388	1.378

TABLE 14

EQUILIBRIUM POTENTIALS FOR H_2/Ni CELL
IN CONCENTRATED ALKALI HYDROXIDE SOLUTIONS
(Charged condition P_{H_2} assumed to be 100 atm)

m/mol kg^{-1}	Temperature/K							
	263	273	298	313	333	353	373	393
LiOH								
1	1.491	1.489	1.482	1.478	1.473	1.467	1.462	1.456
2	1.491	1.489	1.482	1.478	1.473	1.467	1.462	1.456
3	1.491	1.489	1.482	1.478	1.473	1.467	1.462	1.456
4	1.491	1.489	1.482	1.478	1.473	1.467	1.462	1.456
5	1.491	1.489	1.482	1.478	1.473	1.467	1.462	1.456
NaOH								
1	1.491	1.489	1.482	1.478	1.473	1.467	1.462	1.456
2	1.491	1.489	1.482	1.478	1.473	1.467	1.462	1.456
3	1.491	1.489	1.482	1.478	1.473	1.467	1.462	1.456
4	1.491	1.489	1.482	1.478	1.473	1.467	1.462	1.456
5	1.491	1.489	1.482	1.478	1.473	1.467	1.462	1.456
6	1.491	1.489	1.482	1.478	1.473	1.467	1.462	1.456
8	1.491	1.489	1.482	1.478	1.473	1.467	1.462	1.456
KOH								
1	1.491	1.489	1.482	1.478	1.473	1.467	1.462	1.456
2	1.491	1.489	1.482	1.478	1.473	1.467	1.462	1.456
3	1.491	1.489	1.482	1.478	1.473	1.467	1.462	1.456
4	1.491	1.489	1.482	1.478	1.473	1.467	1.462	1.456
5	1.491	1.489	1.482	1.478	1.473	1.467	1.462	1.456
6	1.491	1.489	1.482	1.478	1.473	1.467	1.462	1.456
8	1.491	1.489	1.482	1.478	1.473	1.467	1.462	1.456

Potentials for the Li/air, and to a lesser extent, the Fe/air cells exhibit the opposite behavior. In the case of Li, the decrease in potential with concentration matches the change in the oxygen reduction potentials since the Li anodic reaction is independent of pH. The decrease for Fe is due to a greater shift in the potential of the oxygen reduction reaction with concentration compared with that of the anodic reaction.

The cell potential data for the Fe/Ni system exhibit a different dependence on concentration and temperature from the previous two pairs of systems; an increase in either parameter in this case results in a decrease in the cell potential. The concentration effect, which is small, arises simply from the decrease in the activity of water.

The potential of a H_2/Ni cell is of course strongly dependent on the partial pressure of H_2 and this value reflects the state of charge of the cell. Accordingly, cell potential data were calculated for charged and discharged states. For the charged condition, P_{H_2} was arbitrarily taken as 100 atm while for the discharged condition, P_{H_2} was assumed to be 1 atm. As expected, E_{cell} (charged) is greater than E_{cell} (discharged), with the difference increasing with temperature. However, for both conditions E_{cell} is independent of stoichiometric concentration, and therefore pH, since the pH contributions to the two electrode potentials compensate each other.

Efficiencies

The calculated cell potentials can be used in conjunction with available test data to estimate the efficiencies of the appropriate battery systems. The voltage efficiency of a cell at open circuit can be defined according to equation (3) as

$$\varepsilon_{cell} = \frac{E_{test}}{E_{cell}} \tag{44}$$

where E_{test} is the open-circuit potential for a practical cell and E_{cell} is the computed thermodynamic value. An evaluation of the coulombic efficiencies would require a knowledge of the charge/discharge characteristics for the battery system.

The voltage efficiencies of several systems at open circuit are given in Table 15. In most cases, the potentials of test cells, E_{test}, have been obtained by extrapolation and reading of plotted data, and therefore they are not exact values. In general, the efficiencies of the test cells listed are found to lie between 90-100%. This is a very significant feature since it implies that, at least at open circuit, there is little, if any, contribution from parasitic redox couples to the cell potentials for these systems. The efficiency of the Zn/Ni battery is unexpectedly low, particularly for the 50 Ah cell. However, it should be noted that the value of E_{cell}, and therefore the efficiency of the Zn/Ni system, were obtained assuming $a(Zn(OH)_4^{2-}) = 10^{-6}$ mol kg^{-1}. The use of a higher activity would give a lower E_{cell}, thereby leading to an improvement in the apparent voltage efficiency.

Finally, measured potentials of several electrodes are compared with calculated equilibrium values in Table 16. In the case of Li, the open circuit potential is more positive than the equilibrium potential for the Li/Li^+ couple as a result of the parasitic corrosion reaction (34). Nevertheless, the corrosion potential lies much closer to the potential for the Li/Li^+ couple than that for the H_2O/H_2 couple. This feature indicates that the H_2O reduction is substantially polarised, as noted in earlier work(34), and is therefore the rate-controlling step in the corrosion of Li.

Using polarization data measured previously (31) for the Fe and air electrodes, the open-circuit potentials were obtained by extrapolation to zero current. The open-circuit potential for the Fe electrode is shown to be more positive than the equilibrium potential for the $Fe/Fe(OH)_2$ couple. The air electrode, however, exhibits an open-circuit potential which is considerably less positive than the O_2/H_2O equilibrium potential. These differences would account for the relatively low voltage efficiency found (Table 15) for the Fe/air battery, and furthermore, imply that the major part of the loss in performance is associated with the air electrode. However, in practice H_2O_2 may be the raction product at the air electrode and the potential is therefore determined by the O_2/H_2O_2 couple.

TABLE 15

VOLTAGE EFFICIENCIES OF PRACTICAL BATTERY SYSTEMS AT OPEN CIRCUIT.

System	Ref.	Conditions†	Features*	E_{test}/V	E_{cell}/V	ε/%
H_2/Ni	30	30 $^{w}/_{o}$ KOH, 20°C	P_{H_2} (initial) = 54 atm.	1.46-1.47	1.474	99-100
		8.4A, 7.7Ah Charge	P_{H_2} (final) = 36 atm.	1.34	1.461	91
Fe/air	31	25 $^{w}/_{o}$ KOH + 15g/l LiOH, 44°C, charged at 12.5 mA/cm^2 for 8 hr.	Cell 30, cycle 20, 100 cm^2 electrodes	0.94	1.301	72
Fe/Ni	31	25 $^{w}/_{o}$ KOH, charged at 83.3A/4h	Discharged at 41.7A,	1.43-1.48	1.509	95-98
			83.3A	1.34-1.39		89-92
Zn/Ni	32,33	25 $^{w}/_{o}$ KOH	50 Ah cell,	1.70	2.043#	83
			225 Ah cell	1.83		90

† The temperature was taken as 25°C where not specified. For the Ni/H_2 and Fe/air cells, the values of E_{cell} shown are for 25°C and 40°C, respectively.

* H_2/Ni : The hydrogen partial pressures given are the initial and final values for an open circuit stand of 91.5 hours.

Fe/Ni : The values of E_{test} shown cover a range of cells and cycle numbers.

\# The activity of $Zn(OH)_4^{2-}$ was set equal to 10^{-6} mol kg^{-1}. However, in practice the activity is higher, and therefore E_{cell} would be lower.

TABLE 16

COMPARISON OF OPEN-CIRCUIT ELECTRODE POTENTIALS, E_{oc}

WITH EQUILIBRIUM POTENTIALS, E

Electrode	Ref.	Conditions	Couple	E/V	E_{oc}/V
Li	34	4.5M LiOH, 25°C	Li/Li^+ H_2O/H_2	-3.388* -0.855†	-2.88
Fe	31	25 w/o KOH + 15g/l LiOH, 40°C	$Fe/Fe(OH)_2$	-1.016	-0.95
Air	31	25 w/o KOH + 15g/l LiOH, 40°C	O_2/H_2O#	0.285	0.0

* For the purpose of this comparison, E_{Li/Li^+} for 5m was considered to be adequate. The concentration of Li^+ was set at 10^{-6}m. As the value of m_{Li^+} is increased, E becomes more positive.

† The H_2 partial pressure was taken as 1 atm. A lower pressure would result in a more positive value of E_{H_2O/H_2}.

\# A four electon reaction is assumed. However, the reaction product at the air electrode may be H_2O_2.

Uncertainties in Data Base

It was apparent, when evaluating data in the literature for the properties of concentrated alkaline solutions, that the calculated equilibrium potentials may be subject to considerable error. The principal sources of error are considered to be:

(i) Uncertainty in the activity of water, particularly in the case of concentrated KOH solutions.

(ii) Uncertainty in the dissociation constant for water in concentrated alkaline solutions. This quantity is used to estimate the pH [see equation (18)] but is available only for dilute aqueous solutions (e.g., <1 mol kg^{-1} KCl) over the temperature range of interest.

(iii) Uncertainty in the degree of association of cations with hydroxide ions in the concentrated alkaline solutions. This is of no consequence for the calculation of pH because of the use of the "lever rule" [equation (20)], but will be important when calculating either the concentration or activity coefficient of the hydroxide ion separately.

(iv) Some uncertainty exists in the thermodynamic data base for the dissolved oxidation products of Fe, Ni, Zn, and Al, particularly in the Gibbs energies of formation and heat capacities. These data directly affect the precision of the calculated equilibrium potentials for the metal dissolution reactions, and hence the cell potentials for certain equilibrium cells.

The sources of errors identified above all contribute to the uncertainty in the calculated cell potentials and voltage efficiencies. However, at this time it is not possible to estimate even semi-quantitatively the magnitude of the error for any given system. This will be done in an extension of the work described above which is now underway in this laboratory. Specifically, we are measuring cell potentials for a number of well-behaved equilibrium electrochemical systems involving amalgam (e.g., Hg/K), Hg/HgO, and hydrogen electrodes in concentrated alkaline solutions as a function of temperature.

We expect that these studies will indicate what changes are necessary in the original data base in order to improve the accuracy of the thermodynamic calculations given in this report.

CONCLUSIONS

- The good agreement between the calculated and literature data for the activity coefficient of the hydroxide ion for LiOH, and to a lesser extent for NaOH, indicates that the thermodynamic calculations used to obtain $\gamma_{\pm}$ are sufficiently reliable. The poorer agreement between the $\gamma_{\pm}$ data for KOH may be attributable, at least in part, to inadequate water activity data.

- The properties of the alkali metal hydroxide solutions are very dependent on temperature and concentration of MOH. In particular, the activity of water decreases markedly with increasing concentration, while the dependence of log $\gamma_{\pm}$ on concentration varies with the cation. The pH also depends on the cation and increases along the series LiOH<NaOH<KOH.

- The thermodynamically-favored reaction of the pure metal in the case of Li, Al, and Zn is the desired reaction for the particular battery. The lowest thermodynamically stable product for Fe is FeO_2^{2-} or, at 393K, $HFeO_2^-$. The $Fe/Fe(OH)_2$ reaction would be favored if the activities of FeO_2^{2-} and $HFeO_2^-$ were sufficiently large or the dissolution reactions were discounted for kinetic reasons.

- The relative stabilities of the respective anions for iron (FeO_2^{2-}, $HFeO_2^-$) and zinc ($Zn(OH)_3^-$, $Zn(OH)_4^{2-}$) depend on temperature such that at 393K, each anion in both cases is predominant over a part of the concentration range 1-8 mol kg^{-1}.

- The variation of cell potentials with concentration of MOH and temperature depends on the particular battery. The potentials of the Al/air, Zn/air, and Zn/Ni increase with concentration but decrease as the temperature increases. The Li/air, and to a lesser extent, the Fe/air cell potentials exhibit the opposite behavior whereas those for the Fe/Ni system decrease with an increase in either concentration or temperature. In contrast, the potentials of the H_2/Ni cell are independent of stoichiometric concentration, and therefore pH.

- Efficiencies of H_2/Ni, Fe/Ni, and Zn/Ni test cells at open-circuit lie between 90-100%, implying that there is little, if any, contribution from parasitic redox couples to the open-circuit cell potentials.

- The relatively low efficiency of an Fe/air test battery is associated with the air electrode, suggesting that the potential of this electrode may be determined by the O_2/H_2O_2 couple.

ACKNOWLEDEGMENTS

The authors are grateful for the battery test data provided by G.L. Holleck (EIC Laboratories), B.G. Demczyk (Westinghouse Electric Corporation), H.F. Gibbard (Gould Laboratories) and E.L. Littauer (Lockheed).

REFERENCES

1. G.C. Akerlof and G. Kegeles, J. Am Chem Soc., 62, 612 (1940).
2. R.A. Robinson and R.H. Stokes, Trans. Farad. Soc., 45, 612 (1949).
3. H.S. Harned and F.E. Swindells, J. Am. Chem. Soc., 48, 126 (1926).
4. J. Hinton and E.S. Amis, Chem. Rev., 67, 369 (1967).
5. D.A. Lewis and H.R. Thirsk, Trans. Farad. Soc., 67, 132 (1971).
6. H.S. Harned and B.B. Owen, The Physical Chemistry of Electrolytic Solutions, 2nd Ed., Reinhold, New York (1950).
7. D.D. Macdonald and M.C.H. McKubre, "Temperature Limitations of Alkaline Battery Electrodes. Part II", Final Report to U.S. Dept. of Energy (1979).

8. G.C. Akerlof and H.I. Oshry, J. Am. Chem. Soc., 72, 2844 (1950).

9. F.H. Sweeton, R.E. Mesmer, and C.F. Baes, J. Soln. Chem., 3, 191 (1974).

10. G.B. Naumov, B.N. Ryzhenko, and I.L. Khodakovsky, Handbook of Thermodynamic Data, Transl. U.S. Geological Survey, USGS-WRD-74-001 (1974).

11. K.S. Johnson and R.M. Pytkowicz, Activity Coefficients in Electrolyte Solutions, Vol. II, p. 10, Ed. R.M. Pytkowicz, CRC Press (1979).

12. V.M. Anisimov, Russ. J. Phys. Chem., 47, 601 (1973).

13. P. Bro and H.Y. Kang, J. Electrochem. Soc., 118, 1430 (1971).

14. R.B. MacMullin, J. Electrochem. Soc., 116, 416 (1969).

15. D.D. Macdonald, G. Shierman, and P. Butler, "The Thermodynamics of Metal-Water Systems at Elevated Temperatures. I. The Water and Copper-Water Systems", Atomic energy of Canada Ltd. Report No. AECL-4136 (1972).

16. D.D. Macdonald and P. Butler, Corrosion Sci., 13, 259 (1973).

17. B.G. Pound, D.D. Macdonald, and J.W. Tomlinson, Electrochim. Acta, 24, 294 (1979).

18. C.M. Criss and J.W. Cobble, J. Amer. Chem. Soc., 86, 5385, 5390 (1964).

19. D.D. Wagman, W.H. Evans, V.B. Parker, I. Halow, S.M. Bailey, and R.H. Schum, Selected Values of Chemical Thermodynamic Properties, NBS Technical Note 270-3 (1968).

20. C.E. Wicks and F.B. Block, Thermodynamic Properties of 65 Elements--Their Oxides, Halides, Carbides, and Nitrides, U.S. Bureau of Mines Bulletin 605(1963).

21. P.R. Tremaine, R. Von Massow, and G.R. shierman, Thermochim. Acta, 19, 287 (1977).

22. R.E. Connick and R.E. Powell, J. Chem. Phys., 21, 2206 (1953).

23. P.R. Tremaine, private communication (1979).

24. R.L. Cowan and R.W. Staehle, J. Electrochem. Soc., 118, 557 (1971).

25. B.P. Burylev, Russ. J. Phys. Chem., 47, 1502 (1973).

26. I.L. Kohdakovsky and A. Ye. Yelkin, Geokhimiya, 10, 1490 (1975). Engl. Transl.: Geochemistry International, 127 (1975).

27. M. Pourbaix, Atlas of Electrochemical Equilibria in Aqueous Solutions (NACE, Houston, 1974).

28. H.S. Harned and M.A. Cook, J. Am. Chem. Soc., 59, 496 (1937).

29. R.H. Stokes, J. Am. Chem. Soc., 68, 333 (1946). See also Ref. 6, p. 601.

30. G.L. Holleck, private communication (1982).

31. B.G. Demczyk, private communication (1982).

32. C.C. Chen and H.F. Gibbard, Proc. 14th Intersoc. Energy Conversion Engr. Conf., 725 (1979).

33. H.F. Gibbard and C.C. Chen, private communication (1982).

34. E.L. Littauer and K.C. Tsai, J. Electrochem. Soc., 124, 850 (1977).

APPENDIX A

POLYNOMIAL COEFFICIENTS FOR BEST FIT OF p/p° VS CONCENTRATION FOR LITHIUM HYDROXIDE

T/C°	p/p°			
	A(0)	A(1)	A(2)	A(3)
- 10	0.99264	-0.03085	0.0	0.0
0	1.00059	-0.03177	0.0	0.0
10	0.99759	-0.02636	-0.00096	0.0
20	0.99969	-0.02983	-0.00005	0.0
25	1.00095	-0.03091	0.0	0.0
30	0.99888	-0.02892	0.0	-0.00006
40	1.00048	-0.03012	0.0	0.0
50	0.99980	-0.02971	0.0	0.0
60	0.99975	-0.02909	0.0	0.0
70	1.00004	-0.02881	0.0	0.0
80	0.99996	-0.02845	0.0	0.0
90	1.00317	-0.03524	0.00481	-0.00101
100	1.00137	-0.02905	0.0	0.0
110	1.00195	-0.03062	0.00070	0.0
120	1.00179	-0.02988	0.00050	0.0

POLYNOMIAL COEFFICIENTS FOR BEST FIT OF p/p°
VS CONCENTRATION FOR SODIUM HYDROXIDE

		p/p°		
T/°C	A(0)	A(1)	A(2)	A(3)
- 10	0.98444	-0.01566	-0.00619	0.00025
0	0.98837	-0.01803	-0.00565	0.00023
10	0.98904	-0.01881	-0.00533	0.00021
20	0.98971	-0.01959	-0.00500	0.00020
25	0.98611	-0.01760	-0.00520	0.00021
30	0.99219	-0.02487	-0.00297	0.00001
40	0.99104	-0.02117	-0.00435	0.00017
50	0.99163	-0.02190	-0.00403	0.00016
60	0.99218	-0.02203	-0.00398	0.00016
70	0.99305	-0.02353	-0.00338	0.00014
80	0.99371	-0.02431	-0.00305	0.00012
90	0.99438	-0.02510	-0.00273	0.00011
100	0.99505	-0.02589	-0.00240	0.00009
110	0.99572	-0.02666	-0.00208	0.00008
120	0.99639	-0.02746	-0.00175	0.00007

POLYNOMIAL COEFFICIENTS FOR BEST FIT OF p/p°
VS CONCENTRATION FOR POTASSIUM HYDROXIDE

		p/p°		
T/°C	A(0)	A(1)	A(2)	A(3)
- 10	0.98215	-0.05855	0.0	0.0
0	1.026269	-0.05775	0.0	0.0
20	1.01106	-0.05547	0.0	0.0
25	1.018776	-0.05803	0.0	0.0
40	1.01683	-0.05451	0.0	0.0
60	1.01961	-0.05404	0.0	0.0
80	1.01700	-0.05248	0.0	0.0
100	1.01504	-0.05095	0.0	0.0
120	1.01196	-0.04924	0.0	0.0

Appendices B, C, D and E are too lengthy to permit their inclusion in this report. The appendices are listed as LBID-806. Copies may be obtained upon written request to:

Dr. Frank McLarnon
90-3026
Lawrence Berkeley Laboratory
Berkeley, CA 94720

This report was done with support from the Department of Energy. Any conclusions or opinions expressed in this report represent solely those of the author(s) and not necessarily those of The Regents of the University of California, the Lawrence Berkeley Laboratory or the Department of Energy.

Reference to a company or product name does not imply approval or recommendation of the product by the University of California or the U.S. Department of Energy to the exclusion of others that may be suitable.

TECHNICAL INFORMATION DEPARTMENT
LAWRENCE BERKELEY LABORATORY
UNIVERSITY OF CALIFORNIA
BERKELEY, CALIFORNIA 94720